Biofilm 9 (2025) 100288

Contents lists available at ScienceDirect

Biofilm

journal homepage: www.sciencedirect.com/journal/biofilm

Targeting *Staphylococcus aureus* biofilm-related infections on implanted material with a novel dual-action thermosensitive hydrogel containing vancomycin and a tri-enzymatic cocktail: *in vitro* and *in vivo* studies

Randy Buzisa Mbuku [a,b,c], Hervé Poilvache [b], Loïc Maigret [c], Rita Vanbever [d], Françoise Van Bambeke [b,*,1], Olivier Cornu [a,c,1]

[a] Université catholique de Louvain, Institut de Recherche Expérimentale et Clinique, Neuromusculoskeletal Laboratory, Brussels, Belgium
[b] Université catholique de Louvain, Louvain Drug Research Institute, Pharmacologie cellulaire et moléculaire, Brussels, Belgium
[c] Cliniques Universitaires Saint-Luc, Orthopaedic and trauma Surgery Department, Brussels, Belgium
[d] Université catholique de Louvain, Louvain Drug Research Institute, Advanced Drug Delivery and Biomaterials, Brussels, Belgium

ARTICLE INFO

Keywords:
Biofilm
Vancomycin
Enzymatic cocktail
Poloxamer P407 hydrogel
Implant infection
Tissue cage model

ABSTRACT

Implant-associated infections remain a critical challenge due to the presence of biofilm-forming bacteria, which enhance tolerance to conventional treatments. This study investigates the efficacy of a tri-enzymatic cocktail (TEC; DNA/RNA endonuclease, endo-14-β-D-glucanase, β-*N*-acetylhexosaminidase) targeting biofilm matrix components combined with supratherapeutic doses of antibiotics encapsulated in a thermosensitive hydrogel (poloxamer P407) for local administration. *In vitro,* the hydrogel formulation enabled controlled release of active agents over 12 h. Vancomycin and TEC co-formulated in hydrogel achieved up to 3.8 Log_{10} CFU count reduction and 80 % biofilm biomass reduction on MRSA biofilms grown on titanium coupons, demonstrating enhanced efficacy as compared to individual active agents, with 1.3–3.2 log_{10} additional killing. Fluoroquinolone efficacy remained unchanged by enzyme addition. *In vivo,* in a model of tissue cages containing titanium beads implanted in the back of guinea pigs, hydrogel-delivered vancomycin maintained therapeutic levels for seven days. Coupled with an intraperitoneal administration of vancomycin for 4 days, a single local administration of hydrogel containing both vancomycin and TEC was more effective than hydrogels containing either vancomycin or TEC, achieving an additional 2.1 Log_{10} CFU reduction compared to local vancomycin, 2.3 Log_{10} compared to local TEC, and 4.3 Log_{10} compared to systemic vancomycin treatment alone. However, partial regrowth occurred at later stages, indicating room for further optimization. Nevertheless, these findings already underscore the potential of combining a high dose of antibiotic with an enzymatic cocktail in a sustained-release hydrogel delivery system as a promising strategy for improving the management of biofilm-associated implant infections.

1. Introduction

Implants have become a cornerstone of modern medicine, offering effective solutions for a wide range of medical conditions by restoring impaired biological functions or replacing missing anatomical structures [1]. Ongoing advances in materials and technology have further improved their effectiveness, biocompatibility, and patient outcomes [2,3]. Nevertheless, implant-associated infections (IAIs), including prosthetic joint infections (PJIs), remain a major complication leading to high morbidity and mortality [4] while imposing a substantial burden on healthcare systems [5]. These infections arise when microorganisms adhere to the implant surface and become embedded within an extracellular polymeric matrix, forming a complex three-dimensional microbial biofilm [6]. Biofilms enhance bacterial tolerance to antimicrobial treatments and immune defenses, making infections particularly difficult to eradicate and contributing to their persistence over time [7].

Among the pathogens responsible for PJIs, *Staphylococcus aureus* is one of the most frequently isolated species [8]. The treatment of these infections typically combines prolonged antimicrobial therapy and

* Corresponding author. avenue Mounier 73 b1.73.05 - 1200, Brussels, Belgium.
E-mail address: francoise.vanbambeke@uclouvain.be (F. Van Bambeke).
[1] Equal contribution as last authors.

https://doi.org/10.1016/j.biofilm.2025.100288
Received 3 March 2025; Received in revised form 1 May 2025; Accepted 20 May 2025
Available online 20 May 2025

Table 1
MIC (mg/L) values against MRSA ATCC33591 in two culture media.[a].

Antibiotics	Media	
	MHB-Ca	TGN
Vancomycin	1	8
Ciprofloxacin	0.5	0.5
Moxifloxacin	0.125	0.125

[a] EUCAST breakpoints values (in CA-MHB; mg/L): Vancomycin: S $\leq$ 2; Ciprofloxacin S$\leq(0.001)^2$, R $\geq$ 4; Moxifloxacin S $\leq$ 0.25 [31].

surgery, ranging from implant retention strategies to complete removal, complex reconstructions, or, in severe cases, amputation [9]. Treatment choice depends on several factors, including the type and virulence of the infecting organism, the overall health of the patient, the source and duration of infection, and the implant stability [10]. The Debridement, Antibiotics and Implant Retention (DAIR) strategy is often recommended due to its superior functional outcomes, lower morbidity, and reduced healthcare costs compared to implant replacement [11]. However, DAIR carries a high failure rate (16–57.4 %) [12], largely due to bacterial tolerance to antibiotics within biofilms, underscoring the urgent need for enhanced antibiofilm strategies. Additionally, treating infections in poorly vascularized sites, such as bones and prosthetic devices, poses challenges for systemic antibiotics, making local drug delivery systems a promising alternative [13]. Among these, micro- or nanoparticles loaded with antimicrobials delivered in bone cement or injected in the articulation, prophylactic coatings of the implant as well as hydrogels containing antibiotic-loaded nanoparticles have been described [14]. To date, the co-formulation of antibiotics with large molecules such as enzymes has not yet been reported.

Previous *in vitro* work from our team demonstrated the enhanced activity of a tri-enzymatic cocktail (TEC; DNA/RNA endonuclease, endo-1,4-β-D-glucanase, and β-*N*-acetylhexosaminidase) combined with antibiotics at clinically-achievable concentrations to eradicate biofilm infections caused by a variety of microorganisms (*Escherichia coli*, *Staphylococcus epidermidis,* and *S. aureus*) [15]. However, application of these agents in solution would most likely be inadequate for *in vivo* application due to rapid clearance from the infection site and limited local retention [13]. Therefore, an optimized delivery system is required to maintain therapeutic agents at the infection site without compromising their activity.

Poloxamer 407 (P407) thermosensitive hydrogels meet key criteria for local antibiotic delivery, being biodegradable, biocompatible, well-tolerated, and capable of providing sustained drug release [16,17]. P407 is already widely used for biomedical applications [18]. Existing as a liquid form at low temperatures and transitioning into a gel at body temperature [19], P407 offers a promising platform to effectively target biofilms *in vivo* while minimizing the systemic side effects of active agents.

This study aims to evaluate the efficacy of a combination of the TEC enzymatic cocktail and supratherapeutic concentrations of antibiotics formulated within P407 and administered locally, in order to enable their slow release and sustained local activity. To this end, we first conducted *in vitro* experiments to determine whether the hydrogel formulation of antibiotics and TEC preserves the anti-biofilm activity previously observed in solution [15]. We focused on the reference MRSA strain used in this preliminary work and growing biofilms on titanium alloy surfaces mimicking prosthetic implants. In a next step, we assessed the efficacy of the most effective combination formulated in this hydrogel *in vivo,* using a tissue cage model, in which Teflon perforated cages containing titanium beads simulating prosthetic components were implanted in the back of guinea pigs.

2. Materials and methods

2.1. Bacterial strain

The methicillin-resistant *Staphylococcus aureus* strain ATCC 33591 was used as a representative methicillin-resistant isolate, susceptible to all antibiotics used in this study (Table 1). For *in vitro* experiments, bacteria were streaked from frozen stocks onto Tryptic Soy Agar (TSA) plates and incubated at 37 °C overnight. Fresh colonies were suspended in phosphate-buffered saline (PBS) and adjusted to an OD_{620} of 0.5 (~8.5 $\log_{10}$ CFU/mL) using a CECIL 2021 spectrophotometer (Cecil Instruments Ltd, Milton, UK). For biofilm formation, the suspension was diluted 1:100 in TGN medium (Tryptic Soy Broth + 2 % w/v NaCl + 1 % w/v glucose) [15,20]. For *in vivo* infections, bacterial suspensions were similarly prepared and diluted 1:10 in PBS before injection. The suspension was stored at 4 °C until inoculation (within 2 h). The bacterial inoculum was confirmed by plating serial dilutions on TSA.

2.2. Antibiotics

Ciprofloxacin HCl (potency, 85.9 %) and moxifloxacin HCl (potency, 90.9 %) were supplied by Bayer AG (Leverkusen, Germany). Vancomycin (potency, 97.5 %) was supplied by Mylan (Hoeilaart, Belgium). The antibiotics selected reflect common clinical choices for PJIs and therapeutic realities. Vancomycin is the reference treatment in clinical practice for severe MRSA infections [21,22]. Moxifloxacin is used in specific clinical situations due to its high tissue penetration and residual activity against strains resistant to other antibiotics [23]. Ciprofloxacin, employed empirically in clinical practice, also demonstrates high tissue penetration [24]. Antibiotic concentrations tested were based on the minimal inhibitory concentrations (MIC) of the *S. aureus* ATCC 33591 strain. For *in vitro* assays, vancomycin and moxifloxacin were tested at 10, 100, and 1000x MIC, and ciprofloxacin, at 10, 50, and 100x MIC due to its poor solubility. For *in vivo* experiments, vancomycin powder for intraperitoneal injection was reconstituted with 0.9 % saline at 50 mg/mL, while its final concentration used in the hydrogel for local administration was set to 10 mg/mL (10,000x MIC). This local concentration was chosen to ensure a high local exposure capable of overcoming the protective matrix of biofilms, while remaining within safe limits for localized delivery. Supporting this approach, a study by Sun et al. utilized a vancomycin-loaded *in situ* gelling hydrogel at a concentration of 50 mg/mL, achieving effective antibacterial activity against *S. aureus* without inducing cytotoxicity [25]. Additionally, clinical applications have employed vancomycin at concentrations up to 5 % (50 mg/mL) for local administration without significant adverse effects [26]. These findings suggest that a 10 mg/mL concentration would be both safe and effective for local administration, providing a strong rationale for its use in this study.

2.3. Tri-enzymatic cocktail (TEC)

The tri-enzymatic cocktail (TEC; OrthenzyQure™) used in this study was designed and provided by OneLife SA (Louvain-la-Neuve, Belgium). It consists of a sterile 20 mM Tris-buffered (pH = 7.4) aqueous solution containing 500 U/mL of aspecific DNA/RNA endonuclease from *Serratia marcescens* (c-LEcta GmbH, Leipzig, Germany), 50 U/mL of endo-1,4-β-D-glucanase from *Aspergillus niger* (Sigma-Aldrich, St-Louis, MO), and 10 U/mL of β-*N*-acetylhexosaminidase from *Actinobacillus* sp (Novonesis, Bagsværd, Denmark). Note that the concentration and/or microbial origin of cellulase, denarase, and β-*N*-acetylhexosaminidase in TEC used in this study are slightly different from those previously published [15,27]. This is due to regular optimization of the formulation by OneLife SA. This tri-enzymatic cocktail (TEC) was stored at 4 °C and was heated at 37 °C for 30 min before use. TEC samples are available upon request at OneLife SA for research purposes (under R&D reference OL-R-D1000/OrthenzyQure™). The activity of the cocktail against a

standardized biofilm was evaluated weekly by Onelife SA over six consecutive weeks of storage at 4 °C and found to remain unchanged, demonstrating its stability (Supplementary Figure 1).

2.4. Preparation of a poloxamer 407 hydrogel formulation

Poloxamer 407 was selected as the hydrogel matrix based on its thermosensitive properties, documented biocompatibility, and its ability to release active agents efficiently [17,29]. This last property was confirmed in a preliminary study demonstrating the better performance of P407 over alginate-based hydrogel to release active agents (Supplementary Figure 2).

Poloxamer 407 (P407; Pluronic® F-127) was supplied by Merck KGaA (Darmstadt, Germany). Poloxamer solutions were prepared using a protocol adapted from the "cold method" first described by Schmolka [28]. Briefly, a weighed amount of 2 g of poloxamer 407 was gradually dissolved in 10 mL of cold (4 °C) sterile 20 mM Tris-buffered (pH = 7.4) aqueous solution with gentle stirring. The container was left overnight in a cold room (2°C–4°C) on a roller shaker running continuously at the fixed speed of 30 rpm to ensure complete dissolution, forming a clear, viscous solution.

For hydrogels containing active ingredients, the same process was followed, incorporating antibiotics, combined or not with TEC. These components were added to a sterile 20 mM Tris-buffered (pH 7.4) aqueous solution. The final concentrations in the gel were 0.5, 0.05, and 0.005 mg/mL for ciprofloxacin; 1.25, 0.125, and 0.0125 mg/mL for moxifloxacin; and 10, 1, and 0.1 mg/mL for vancomycin. All poloxamer-containing solutions were sterilized by filtration using 0.22 μm pore size filters at 4 °C.

2.5. Rheological characterization of P407-based formulations

Rheological analyses were performed to assess the impact of active agent incorporation on the gelation properties of P407. Rheological parameters were measured using a stress-controlled rotational rheometer (MCR102; Anton-Paar, Graz, Austria) under oscillatory mode in plate-plate geometry (plate diameter 40 mm; Gap 0.076 mm) with a linear temperature ramp (10 °C–40 °C at 1 °C/min, 1 Hz, 0.1 % strain). The following parameters were examined. (i) The gelation temperature (Tgel), defined as the temperature at which G′ (storage modulus) crosses G″ (loss modulus), indicates the thermosensitive transition point from liquid to gel. (ii) The plateau G′ value (35.5°C-38.5 °C) provides insight into gel consistency over physiological temperature ranges [30]. (iii) The gelation kinetics (ΔG'/ΔT), calculated a window of [T°gel +2°], quantifies the rate of network formation, which can influence *in situ* retention.

2.6. Antibiotic susceptibility testing

MICs were determined by microdilution following the European Committee on Antimicrobial Susceptibility Testing (EUCAST) guidelines [31] in cation adjusted Mueller-Hinton broth (MHB-Ca, Sigma-Aldrich) and TGN (Tryptic Soy Broth [VWR Chemicals, Leuven, Belgium] + 2 % w/v NaCl + 1 % w/v glucose), i.e., the medium used for growing biofilm [15].

2.7. In-vitro release kinetics of active ingredients from poloxamer 407

One mL of poloxamer solution containing an antibiotic and/or the TEC enzymatic cocktail was placed in 15 mL conical tubes and allowed to jellify at room temperature. Nine mL of sterile tris-HCl buffer was then added and the tubes were incubated at 37 °C. Five hundred μL aliquots were collected at hourly intervals for the first 8 h, followed by additional collections at 12, 24, 48, and 72 h. Volume was readjusted to initial volume (10 mL) with fresh buffer after each sampling. Antibiotic concentrations were determined at each time point using validated methods adapted to each molecule. For vancomycin, we used a disk diffusion bioassay against *S. aureus* ATCC 25923 MSSA as test organism. The diameter of the inhibition zone was converted to concentration using a calibration curve established with vancomycin standards of known concentration. For ciprofloxacin and moxifloxacin, fluorescence-based quantification was performed using a SpectraMax M3 spectrophotometer (excitation/emission: 278/450 nm) [32] (Molecular Devices, San Jose, CA), exploiting the intrinsic fluorescence of fluoroquinolones. The concentrations were calculated using a standard curve prepared in the same buffer. Enzymatic concentrations were measured using the Pierce™ BCA protein assay (Thermo Fisher Scientific Inc., Waltham, MA), following the microplate protocol of manufacturer. Absorbance was read at 562 nm using a SpectraMax M3 and compared to a BSA standard curve.

2.8. Anti-biofilm activity in vitro

Biofilm formation. Biofilms were grown on titanium alloy (Ti–6Al–4V) coupons (BioSurface, Bozeman, MN, USA) placed in 24-well plates and covered by 1 mL of the final bacterial suspension. The plates were incubated for 24 h at 37 °C, with a constant orbital shaking of 50 rpm. Those growth conditions were previously shown to allow *S. aureus* biofilm to reach a steady-state over the study period [33].

Biofilm treatments. All coupons were then washed twice in sterile PBS and transferred to 6-well plates containing either 10 mL of TGN-media (control) or 9 mL of TGN supplemented with 1 mL of different treatment solutions: Tris-HCl buffer (pH = 7.4) with antibiotic solution or enzymatic cocktail, or their combination, or 1 mL of preformed hydrogel P407 without active agents, P407 containing antibiotics or the enzymatic cocktail, or their combination. Plates were then reincubated for 24 h at 37 °C under a constant orbital shaking of 50 rpm.

Biofilm quantification. Treated coupons were washed twice in sterile PBS and remaining biofilm was quantified as follows [15]. ***(i) Biofilm CFU counts.*** Coupons were placed in 15-mL conical tubes (Greiner Bio-One International GmbH, Kremsmünster, Austria) containing 3 mL of sterile PBS. In order to detach the biofilms and suspend the bacteria, the tubes were then vortexed for 30s at maximum intensity (Vortex-Genie 2; Scientific Industries, Inc., Bohemia, NY, USA), sonicated for 5 min in an ultrasonic bath (Branson 5510 Ultrasonic bath, Emerson Electric, Saint-Louis, MO, USA) at a frequency of 42 kHz and a power of 130 W, and then vortexed again for 30 s. The suspension was then sampled and serially diluted before plating on TSA. After 16h incubation at 37 °C, CFU were counted using an automated method (image acquisition using Gel Doc XR1 and image processing using Quantity One (Bio-Rad, Hercules, CA, USA). ***(ii) Biomass quantification***. Coupons were dried at 60 °C overnight. They were then stained with 1 mL of 1 % crystal violet solution for 10 min at room temperature (Sigma-Aldrich Corp.), washed twice using deionized water to remove the excess dye and then placed for 1 h in 24-well plates filled with 1 mL of 66 % acetic acid solution at room temperature (Merck KGaA, Darmstadt, Germany) to resolubilize the dye. Absorbance of the solution was read at 570 nm using a SpectraMax M3 spectrophotometer.

Fluorescence confocal microscopy with live-dead staining. Coupons were rinsed twice in sterile deionized water to avoid interference from phosphate ions. They were then stained using the Filmtracer LIVE/DEAD biofilm viability kit (Thermo Fisher Scientific Inc.) according to the manufacturer's instructions. Coupons were then rinsed again twice in sterile deionized water before imaging using an Axio Imager Z1 microscope fitted with an ApoTome 1 attachment (Zeiss, Oberkochen, Germany) at a x20 magnification. The images were postprocessed using the FIJI software [34] and the maximum intensity projection technique, and by adjusting the brightness of the channels.

Biofilm-associated bacterial coverage and viability were analyzed from 2D confocal images (single optical plane, 1024 × 1024 pixels, 20 × magnification) using FIJI/ImageJ software [34]. For each experimental group, three to six independent fields were analyzed. The green (SYTO

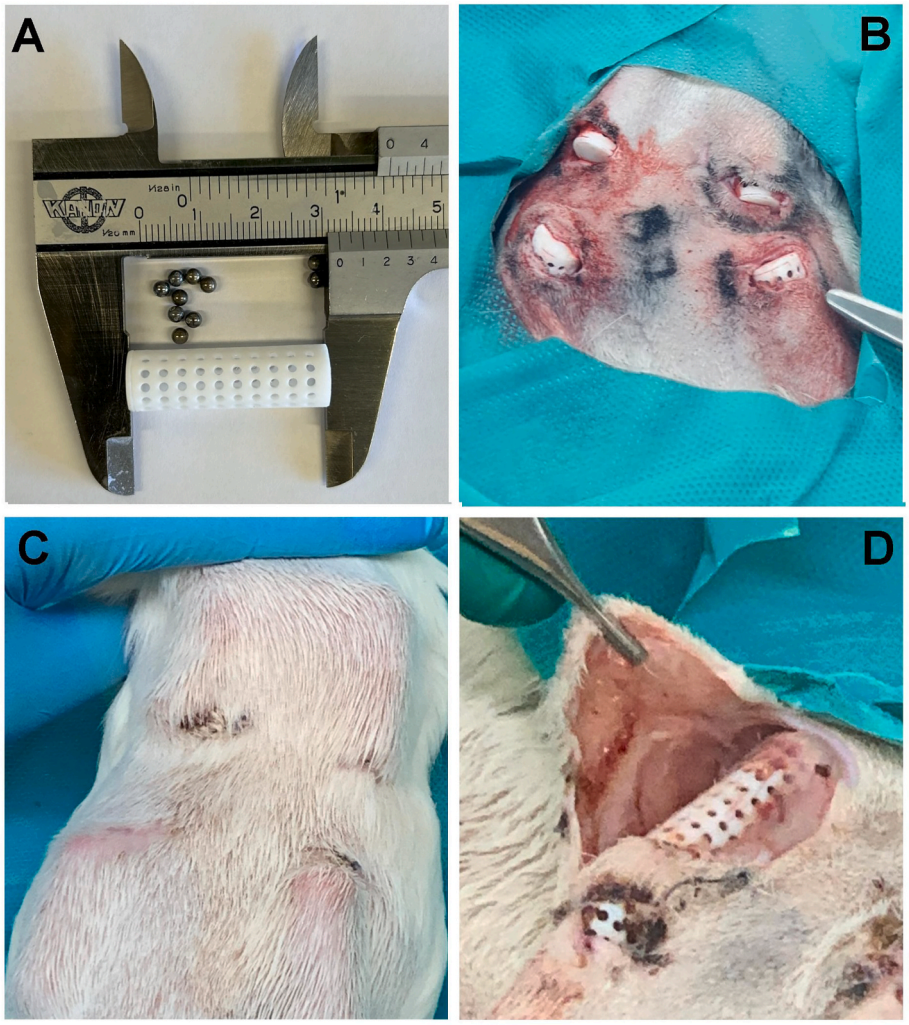

Fig. 1. Illustration of the in vivo model. **(A)** Ti–6Al–4V beads (up) and Teflon cage (down). **(B)** Per-operative view. **(C)** 14-day postoperative view. **(D)** Explantation post-mortem view.

9, live bacteria) and red (propidium iodide, dead bacteria) fluorescence channels were separated, and average intensity projections were generated for analysis to avoid overrepresentation of dense regions associated with maximum intensity projection. For each channel, the integrated density (i.e., product of fluorescence-positive area and mean intensity) was calculated. The green/red intensity ratio was used as a surrogate marker of bacterial viability. In parallel, the surface area covered by each signal (red and green) was quantified using the Otsu thresholding method [35], and expressed as a percentage of the total fluorescent area, serving as a proxy for bacterial coverage. The total surface colonization (red + green) was also calculated and normalized to the untreated control group (TGN). All image analyses were performed under identical thresholding parameters and blinded to the treatment groups.

Fluorescence confocal microscopy for EPS (Extracellular Polymeric Substances) composition (eDNA and polysaccharides). To assess the composition of the biofilm extracellular matrix, additional confocal fluorescence imaging was performed to detect extracellular DNA (eDNA) and polysaccharides. Biofilms grown on titanium coupons were exposed to the same experimental conditions as described previously (TGN, TEC, vancomycin [VAN] as antibiotic, or the combination of VAN and TEC). Following treatment, samples were stained with 2 μL of TOTO-1 iodide (1 mM stock in DMSO; Thermo Fisher Scientific Inc.) to label extracellular DNA (eDNA), and 2 μL of a mixture of Calcofluor White M2R (commercial 1 % solution = 10 mg/mL; Sigma-Aldrich) and Evans Blue (commercial 0.5 % solution = 5 mg/mL; Sigma-Aldrich) to detect β-linked polysaccharides [36], then imaged with a 40x objective using a Zeiss Axio Imager Z1 microscope equipped with Apotome. Three independent fields were acquired per sample. Image processing and quantitative analysis were performed using FIJI (ImageJ). For each fluorescence channel (TOTO-1 and CFW-EB), Z-stacks were processed using average intensity projections to account for the overall spatial distribution and volumetric extent of matrix components across the biofilm depth. This approach was chosen over maximum projection to better reflect the total matrix burden, minimizing the influence of high-intensity outliers and providing a more integrated measurement of biofilm architecture. Otsu [35] thresholding was applied for segmentation, and quantification was performed using the "Analyze Particles" plugin, with a minimum object size of 10 pixels^2 to exclude background noise. The percentage of area covered (%Area) was recorded for each field and condition.

2.9. Antibiofilm activity in vivo

Animal model. We used the tissue cage guinea pig model established by Zimmerli et al. [37]. The animal experiments were performed with the approval of the local ethics committee (2022/UCL/MD/26). After a 7-days acclimatization period, four sterile cylindrical polytetrafluoroethylene "Teflon" tissue cages (10 by 32 mm and perforated with 130 holes) (Europlex, Nivelles, Belgium) containing 10 titanium alloy

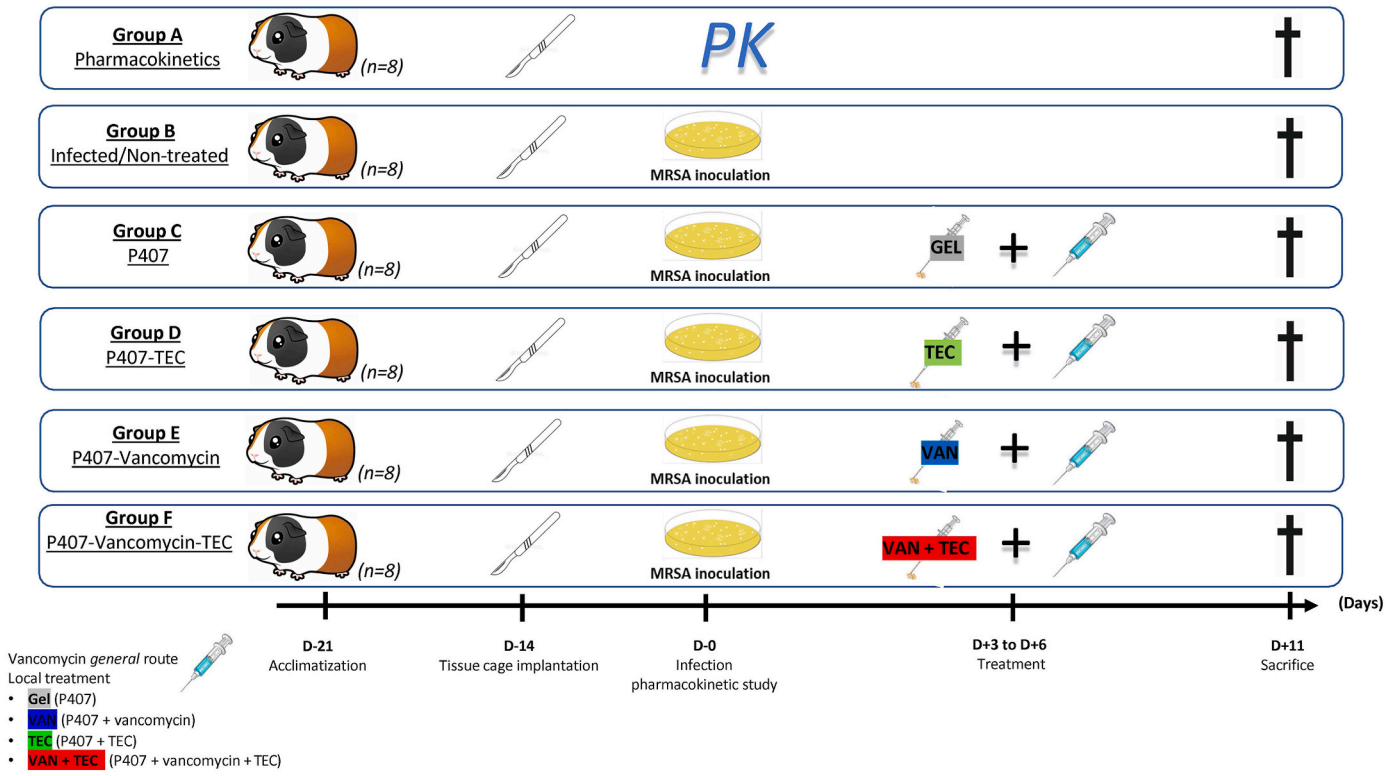

Fig. 2. Study design. Animals were assigned to six groups six groups: vancomycin pharmacokinetics (group A), infected/non-treated (group B), infected/treated locally in cages with P407 (group C), with P407 containing TEC (group D), with P407 containing vancomycin at 10 mg/mL (group E) and with P407 containing their combination (group F).

beads (Ti–6Al–4V; 3 mm diameter) per cage, were aseptically implanted in the back of guinea pigs weighting 450–600 g. The animals were anesthetized with an intraperitoneal injection of ketamine 50 mg/kg (Nimatek®, Dechra Pharmaceuticals PLC, Norwich, United Kingdom) and xylazine 5 mg/kg (Rompun®, Bayer AG, Leverkusen, Germany). The experiments were started after complete wound healing (i.e., approximately 2 weeks after surgery) (Fig. 1). Before each experiment, the cages were checked for sterility by culturing the aspirated cage fluid (TCF; 150–300 μL) for 7 days. A total of 48 female guinea pigs were randomly assigned to six groups: vancomycin pharmacokinetics (A), infected/non-treated (B), infected/treated locally in cages with P407 (C), with P407 containing TEC (D; TEC in P407), with P407 containing vancomycin at 10 mg/mL (E; VAN in P407) and with P407 containing their combination (F; VAN + TEC in P407) (Fig. 2).

Vancomycin pharmacokinetics. Vancomycin concentrations were measured at preset time points (30 min, 1, 3, 6, 9, and 12 h) in serum and TCF of non-infected animals (group A) following a single intraperitoneal dose of vancomycin (15 mg/kg). Additionally, 5 days later (after washing the cages with saline solution), animals received 1 mL of P407 containing vancomycin (10 mg/mL) and TEC locally into the cages and their concentrations were measured at 30 min, 1, 3, 6, 9, 12, 24, 96, 144, and 168 h in serum and TCF. Aliquots (150–300 μL) of all samples were transferred to Eppendorf tubes and centrifuged at 2500 *g* for 15 min, and supernatants were stored at −20 °C until further analysis. For local injection, vancomycin concentrations were quantified using disk diffusion method with *S. aureus* strain ATCC 25923 MSSA as test organism as described earlier. For intraperitoneal injections, vancomycin concentrations in serum and TCF were measured using the Roche VANC3 assay on a COBAS 8000 automated analyzer (Roche Diagnostics GmbH, Mannheim, Germany).

Infection and treatment efficacy. Cages were infected with the MRSA ATCC 33591 strain by percutaneous injection of 200 μL bacterial suspension in each cage (day 0). Infection was confirmed by quantitative culture of TCF fluid at day 3. Animals in group B were not treated. Animals in groups C, D, E, and F received a single local injection (into cages) of 1 mL of P407, with or without active agents, followed by intraperitoneal injection of vancomycin at 15 mg/kg every 12 h for 4 days (days 3–6). To assess the efficacy of the treatment against planktonic bacteria, TCF samples were taken at preset times (day 3, 4, 7, 9 and 11) from all animals. Samples were placed in 500-μL conical Eppendorf-tubes, vortexed at maximum intensity 30 s, serially diluted in PBS, and then plated on TSA for bacterial quantification. The efficacy of the treatment against adherent bacteria was assessed using implanted materials removed from euthanized animals 24 h after the start of treatment, 24 h after the end of treatment, and at the end of the follow-up period. These samples were placed in 15-mL conical tubes containing 5 mL of sterile PBS, vortexed at maximum intensity for 30 s, sonicated for 5 min (Branson 5510 Ultrasonic Bath, Emerson Electric, Saint Louis, MO), and vortexed again for 30 s to dislodge adhering bacteria.

Leucocytes count. TCF samples were collected in 500-μL Eppendorf-tubes and diluted 20-fold in Türk's solution (3 % acetic acid, 0.01 % crystal violet in mQ water). After 5 min, 10 μL of the diluted samples were placed in a Bürker counting chamber (Paul Marienfeld GmbH & Co. KG, Lauda-Königshofen, Germany), and cells in 4 large squares were counted by a blinded observer.

Postoperative follow-up. The pain level of the animals and their general condition were monitored daily using a standardized guinea pig pain scoring system [38], adapted from rodent welfare guidelines. The followed parameters included general appearance, spontaneous activity, social interaction, food and water intake, and wound inspection. Each criterion was scored from 0 (normal) to 3 (severely altered), with a maximum cumulative score of 15. Animals were euthanized if they scored 3 in any single category or ≥6 overall. Body weight was measured two days post-surgery and weekly thereafter (Supplementary Figure 3); a loss >20 % was also considered a humane endpoint. Postoperative analgesia consisted of meloxicam (0.4 mg/kg, subcutaneous, once daily

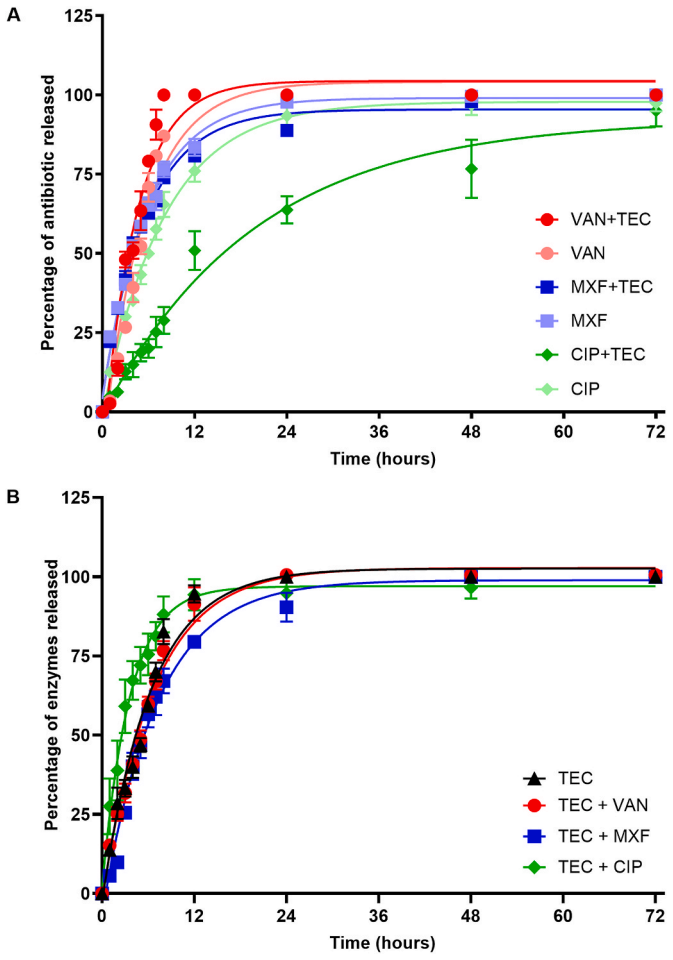

Fig. 3. Kinetics of release of active agents from P407 hydrogel. In vitro release kinetics of antibiotics and enzymes from 2 g/10 mL poloxamer 407 hydrogel in a TRIS-HCl buffer 20 mM at pH 7.4. **(A)** antibiotic release: vancomycin (VAN; red circles; initial concentration 10 mg/mL), moxifloxacin MXF: blue squares; initial concentration 1.25 mg/mL) or ciprofloxacin (CIP; green diamonds; initial concentration 5 mg/mL), alone (light color symbols) or combined with TEC (dark color symbols). **(B)** TEC release: TEC alone (black triangles) or combined with vancomycin (red circles), moxifloxacin (blue squares) and ciprofloxacin (green diamonds). Values are means ± standard deviation of triplicate (n = 3). (For interpretation of the references to color in this figure legend, the reader is referred to the Web version of this article.)

for 3 days).

2.10. Data transformation and statistical analysis

The release kinetics data were analyzed using nonlinear regression. The combined effect of TEC and antibiotics was assessed separately for *in vitro* and *in vivo* models. In the *in vitro* model, a one-way ANOVA was used after checking for normality with QQ plots and variances with the Levene test, while in the *in vivo* model, a two-way ANOVA was performed. Pairwise comparisons were made using the Tukey or Dunnett Honestly Significant Difference (HSD) test. Vancomycin serum AUCs were calculated using the trapezoid rule. Interaction between treatments was assessed through ANOVA [39]. The threshold for alpha errors was set at 0.05. Data are reported as means with 95 % confidence intervals (CI) or medians with 95 % CI obtained through bootstrapping. All statistical analyses were conducted using GraphPad 9.4.1 (GraphPad Software Inc., San Diego, CA, USA).

Table 2
Parameters of release kinetics of active agents from P407. Constant rate K (h^{-1}) and half-time $t_{1/2}$ (h).

Active agents in P407	Parameters			
	K (h^{-1})	p-value	Half-life (h) [95 % CI]	AUC (μg.h.ml^{-1}) [95 % CI]
Antibiotics				
Vancomycin (VAN)				
alone	0.18	0.03	3.78 [3.59; 4.37]	6707 [6690; 6725]
with TEC	0.23		3.00 [2.56; 3.52]	6798 [6777 to 6820]
Ciprofloxacin (CIP)				
alone	0.13	<0.0001	5.53 [4.98; 6.16]	6189 [5858; 6521]
with TEC	0.08		13.73 [10.45; 19.05]	4710 [4094; 5325]
Moxifloxacin (MXF)				
alone	0.17	0.62	4.06 [3.72; 4.42]	6548 [6481; 6615]
with TEC	0.18		3.93 [3.59; 4.31]	6315 [6284; 6347]
Enzymatic cocktail				
TEC				
alone	0.16		4.37 [3.86; 4.96]	6655 [6588; 6722]
with VAN	0.15	0.28	4.61 [4.17; 5.11]	6644 [6528; 6761]
with CIP	0.28	<0.001	2.54 [2.00; 3.12]	6621 [6290; 6951]
with MXF	0.14	0.07	4.94 [4.33; 5.67]	6277 [6063; 6490]

Concentration of active agents in Poloxamer 407: vancomycin 10 mg/mL, ciprofloxacin 0.5 mg/mL, moxifloxacin 1.25 mg/mL and enzymes cocktail TEC (400 U/mL of aspecific DNA/RNA endonuclease, 50 U/ml of endo-1,4-b-D-glucanase and 2,6 U/ml of β-N-acetylhexosaminidase).

3. Results

3.1. Antimicrobial susceptibility testing

MICs against MRSA ATCC33591 are shown in Table 1. The strain was susceptible to all antibiotics tested in CA-MHB; however, the vancomycin MIC was 3 doubling-dilutions higher when tested in TGN, consistent with previous observations from our laboratory [15].

3.2. Release kinetics of active agents from P407 in vitro

We first investigated the kinetics of release of active agents from P407. A high proportion of all active agents (≥75 %) were released within the first 12 h (Fig. 3; Table 2). Regarding antibiotics (Fig. 3A), vancomycin (VAN) was fully released in 12 h when loaded alone (κ: 0.18 h^{-1} and $t_{1/2}$ 3.7 h), and in only 8 h when co-formulated with TEC. Moxifloxacin (MXF), whether alone or combined with TEC, exhibited a similar initial rate similar to vancomycin, but reached a near-complete release only after 24 h. Ciprofloxacin (CIP) was not fully released after 72 h, regardless of co-formulated with TEC. However, its release was reduced in the presence of enzymes. Complete release of TEC was observed within 24 h and was unaffected by the presence of antibiotics, except for ciprofloxacin, which accelerated enzyme release (Fig. 3B).

3.3. In vitro anti-biofilm activity of antibiotics, TEC, and their combination formulated in P407 or in solution

Based on these favorable release profiles, we next assessed whether formulating the active agents in P407 influenced their activity. MRSA

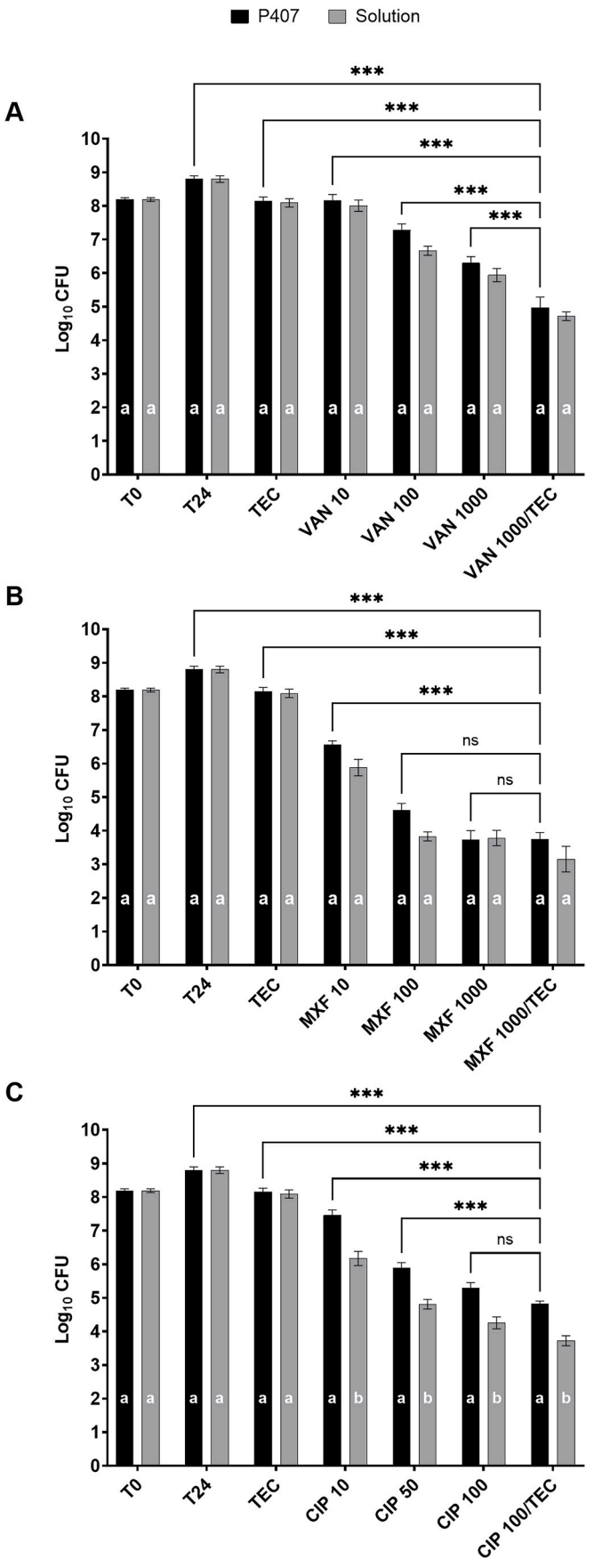

(caption on next column)

Fig. 4. Activity of antibiotics and TEC in vitro. CFU (in Log_{10} per coupon) in biofilms of MRSA ATCC33591 at the time of drug addition (T0), or after 24 of incubation in control conditions (T24) or in the presence of TEC alone, antibiotic alone at the indicated concentrations in x of their MIC ((**A**): vancomycin; VAN 0.1, 1, 10 mg/mL; (**B**) moxifloxacin; MXF 0.0125, 0.125, 1.25; (**C**) ciprofloxacin, CIP 0.05, 0.25, 0.5 mg/mL) or the combination of the antibiotic at the highest concentration tested + TEC. The active agents are formulated in Poloxamer 407 hydrogel (20 % w/v) or Tris-HCl buffer (20 mM, pH 7.4) (black bars) or in solution (grey bars). Values are the mean ± standard error from triplicate experiments performed in three replicates. Distinct letters indicate statistically significant differences when comparing the two formulations (Poloxamer 407 vs. solution). Statistical analysis: two-way ANOVA with Tukey HSD, comparing different treatments in a same formulation (*$p < 0.05$; **$p < 0.01$; ***$p < 0.001$).

biofilms grown on titanium coupons were exposed to increasing concentrations of antibiotics over 24h, either alone or in combination with TEC, formulated in solution or within P407. The effect of these treatments on biofilm culturability (CFU) and biomass are shown in Figs. 4 and 5, respectively.

Overall, no statistically significant differences in CFU counts were observed when comparing solution or hydrogel formulations, except for ciprofloxacin which exhibited slightly greater activity in solution (Fig. 4). TEC alone did not affect CFU counts. Antibiotics alone showed concentration-dependent reduction in CFU counts. The combination of TEC and vancomycin proved more effective than the individual agents, resulting in an additional 1.3 Log_{10} reduction in CFU counts ($p < 0.001$) compared to vancomycin alone, a 3.2 Log_{10} reduction ($p < 0.001$) compared to TEC alone, and a 3.8 Log_{10} reduction compared to control (T24). Combining TEC with ciprofloxacin or moxifloxacin in hydrogel at the highest concentration tested reduced CFU counts by 3.3 Log_{10} ($p < 0.001$) and 4.4 Log_{10} ($p < 0.001$), respectively, compared to TEC alone; these effects are similar to those observed for the antibiotic alone, indicating that the adjunction of TEC did not improve fluoroquinolones activity against biofilms.

In terms of biomass reduction (Fig. 5), no statistical difference was seen between solution and hydrogel formulations across all conditions tested. The effect of antibiotics was concentration-dependent, with reductions ranging from 48 % to 51 % (vancomycin or ciprofloxacin) to 65 % (moxifloxacin) at the highest concentration tested. TEC alone achieved a 71.3 % reduction ($p < 0.001$). The combination of TEC and vancomycin resulted in a 31.7 % reduction ($p < 0.01$) compared to vancomycin alone and by 8.7 % (ns) compared to TEC alone in hydrogel. Similarly, TEC combined with ciprofloxacin reduced biomass by 22.5 % compared to ciprofloxacin alone and by 1.8 % compared to TEC alone in hydrogel. The biomass reduction with the TEC and moxifloxacin combination was 25.2 % and 12.2 % greater compared to moxifloxacin alone or TEC alone, respectively. However, these differences with fluoroquinolones or TEC alone did not reach statistical significance.

Given the enhanced efficacy observed with the vancomycin–TEC combination in reducing both CFU counts and biofilm biomass *in vitro* and the privileged use of vancomycin against MRSA infections in the clinics, this combination was selected for (i) further *in vitro* characterization and (ii) *in vivo* evaluation, in a model of biofilm-infection on material implanted in guinea pigs.

3.4. Confocal microscopy imaging of biofilms exposed to P407-based formulations containing vancomycin, TEC, or their combination

Confocal fluorescence microscopy following LIVE/DEAD staining corroborated the CFU and biomass assay results for the VAN-TEC combination, demonstrating a marked reduction in viable cells as evidenced by decreased green fluorescence intensity (Fig. 6). Quantitative analysis of confocal images revealed a significant decrease in the surface area colonized by bacteria after treatment. Compared to the untreated control (TGN), TEC reduced surface coverage by ~25 %, VAN by ~70 %,

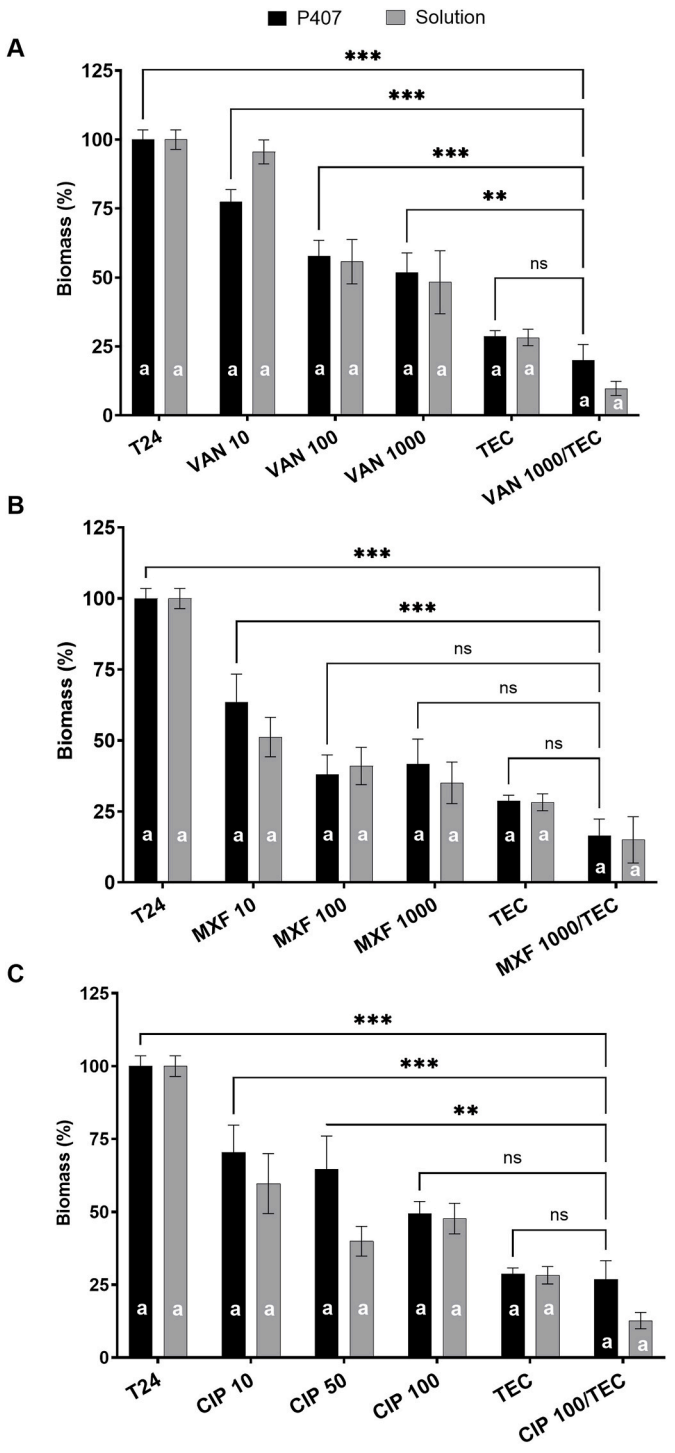

Fig. 5. Activity of antibiotics and TEC in vitro. Biofilm biomass (in percentage of value measured at time 0) in biofilms of MRSA ATCC33591 at the time of drug addition (T0), or after 24 of incubation in control conditions (T24) or in the presence of antibiotics alone at the indicated concentrations in x of their MIC ((**A)** vancomycin; VAN 0.1, 1, 10 mg/mL; (**B)** moxifloxacin; MXF 0.0125, 0.125, 1.25; **(C)** ciprofloxacin, CIP 0.05, 0.25, 0.5 mg/mL), TEC alone, or the combination of the antibiotic at the highest concentration tested + TEC. The active agents are formulated in Poloxamer 407 hydrogel (20 % w/v) or Tris-HCl buffer (20 mM, pH 7.4) (black bars) or in solution (grey bars). Values are the mean ± standard error from triplicate experiments performed in three replicates. Distinct letters indicate statistically significant differences when comparing the two formulations (Poloxamer 407 vs. solution). Statistical analysis: two-way ANOVA with Tukey HSD, comparing different treatments in a same formulation (*$p < 0.05$; **$p < 0.01$; ***$p < 0.001$).

and the VAN-TEC combination by ~95 %. The difference between VAN-TEC and individual therapies was statistically significant ($p < 0.05$ to $p < 0.001$), confirming the superior efficacy of the combined enzymatic and antibiotic treatment in reducing biofilm coverage (Fig. 6B). To further evaluate bacterial viability, the proportions of live (green) and dead (red) cells were assessed using a percentage area approach (Fig. 6C). In the TGN group, the majority of the biofilm signal originated from live bacteria (~90 %). TEC induced a modest reduction in viability (~23 % red), which did not reach statistical significance versus control (ns). VAN significantly increased the dead cell fraction (~48 %, $p < 0.01$ vs TEC), while the VAN-TEC combination resulted in a striking predominance of red signal (~80 %), significantly higher than that observed in all other groups ($p < 0.0001$ vs TGN, $p < 0.05$ vs VAN). These results indicate that while enzymatic treatment alone has limited bactericidal effect, its combination with vancomycin enhances killing efficacy, likely due to improved antibiotic activity following biofilm matrix disruption.

To further explore the effect of TEC and VAN treatments on biofilm architecture, we quantified two major components of the extracellular polymeric substances (EPS): extracellular DNA (eDNA) and polysaccharides (CFW signal). Representative confocal images (Fig. 7) revealed a substantial reduction in both signals in the TEC and VAN-TEC groups compared to untreated biofilms (TGN). Quantification was performed on average intensity projections of Z-stacks to capture the full volumetric contribution of matrix material across the biofilm thickness. This method provides a robust estimate of total matrix presence, integrating both distribution and intensity. TEC alone led to a decrease of 65 % in eDNA and 48 % in polysaccharides area coverage, while VAN-TEC reduced eDNA and CFW signals by 70 % and 57 %, respectively. VAN alone showed a moderate effect (−39 % eDNA, −20 % CFW). These results were consistent across average and maximum values per field, underscoring the matrix-degrading effect of the enzymatic cocktail.

3.5. Rheological characterization of P407-based formulations containing vancomycin, TEC, or their combination

We conducted a comprehensive rheological characterization of P407 hydrogels as a final preliminary to in-vivo experiments to determine whether the incorporation of VAN, the trienzymatic cocktail TEC, or their combination (VAN-TEC) altered its thermoresponsive properties. As shown in Fig. 8 (and Supplementary Fig. 4 for more details), temperature ramp experiments revealed that VAN increased the sol-gel transition temperature (Tgel) of P407 from 24.5 °C to 26.5 °C ($p < 0.05$), while both TEC and VAN-TEC reduced it from 24.5 °C to 22 °C ($p < 0.05$), bringing gelation onset closer to ambient temperature. This shift suggests a need for refrigerated storage and immediate injection upon removal from refrigeration to prevent warming and premature gelling before administration. Despite this decrease in Tgel, the storage modulus at physiological temperature (G′ at 37 °C) remained in the kilopascal range for all formulations, indicating that the gel achieved adequate mechanical stiffness after full transition. The elastic modulus (average G′ between 35.5 and 38.5 °C) reduced in all loaded formulations, particularly with TEC and VAN-TEC, suggesting a moderate decrease in gel solidity. As elasticity reflects resistance to deformation, these findings indicate that gels containing active agents might be more susceptible to mechanical stress. Regarding the gelation kinetics, defined by the slope $\Delta G'/\Delta T$ around Tgel, P407 exhibited the steepest slope (166 Pa/°C), consistent with a sharp gelation transition. VAN, and to a much larger extent, TEC and VAN-TEC significantly reduced this slope, indicating a more gradual gelation process that could translate into delayed *in situ* formation under physiological conditions.

Altogether, these data suggest that while P407 remains a biocompatible and thermoresponsive platform, the incorporation TEC alone or combined with VAN slightly lowers the gelation temperature, reduces the mechanical stiffness of the gel, and flattens the gelation slope, leading to a slower, more progressive sol–gel transition.

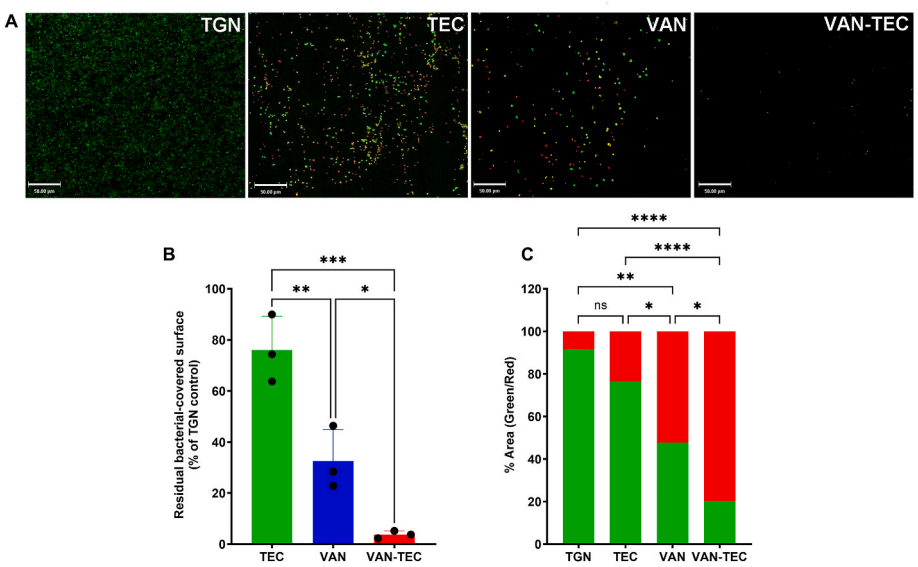

Fig. 6. Confocal microscopy and quantitative analysis of surface colonization and viability in MRSA biofilm. (A) Representative confocal microscopy images of mature MRSA ATCC33591 biofilm grown for 24 h in TGN (control), or in the presence of poloxamer 407 hydrogel (20 % w/v) containing TEC and/or vancomycin (VAN, 10 mg/mL). Green: live bacteria (SYTO 9); red: dead bacteria (propidium iodide). Scale bars: 50 μm. **(B)** Residual surface area colonized by bacteria (SYTO 9 + PI signal), expressed as a percentage of the untreated TGN control. This measurement reflects the extent of bacterial attachment on the surface. **(C)** Percentage of surface covered by live (green) and dead (red) bacteria. This analysis enables visualization of treatment-induced shifts in bacterial viability. Images were acquired at 20 × magnification. Data represent mean ± SEM from three independent fields per condition. Statistical analysis by one-way ANOVA followed by Tukey's test. *$p < 0.05$; **$p < 0.01$; ***$p < 0.001$; ****$p < 0.0001$; ns: not significant. (For interpretation of the references to color in this figure legend, the reader is referred to the Web version of this article.)

3.6. Vancomycin pharmacokinetics in vivo

As a preliminary step in evaluating the treatment efficacy, we first examined the pharmacokinetic profile of vancomycin in non-infected animals after a single dose given either intraperitoneally or injected into tissue cages in hydrogel formulation (group A). Fig. 9 (**panels A and B**) illustrates the concentration-time curves of vancomycin in serum and sterile TCF after the administration of a single intraperitoneal dose of 15 mg/kg. Tables 3 and 4 summarize the values of the calculated pharmacokinetic parameters. The peak concentration (C_{max}) in TCF was delayed by 2h30 compared to serum. Moreover, both the peak concentration (C_{max}) and the Area Under the Curve (AUC) were approximately 4.4-fold and 2-fold lower in TCF compared to serum. The half-life ($T_{1/2}$) in TCF was nearly 5 times longer than that observed in serum.

The local pharmacokinetic profile of vancomycin released from P407 formulation containing 10 mg/mL of antibiotic and injected in tissue cages is shown in Fig. 9C. The local vancomycin concentration decreased from 984 μg/mL after 30 min, to 300 μg/mL after 12 h, then to 79.7 μg/mL after 24 h. Local levels remained therefore higher than the minimal inhibitory concentrations for MRSA ATCC33591 (1 μg/mL in MHB-Ca or 8 μg/mL in TGN [15]) throughout the experiment (>20 μg/mL and 10 μg/mL, after 4 and 7 days, respectively). The $AUC_{0–168h}$ calculated after the local injection of vancomycin into the cage was approximately 210 times higher than that observed in the tissue cage fluid following a single intraperitoneal dose of 15 mg/kg vancomycin. Vancomycin concentration was undetectable in serum following the local injection.

3.7. Infection profile in Guinea pigs

A second group of animals (group B) was used to follow the course of the infection in the absence of treatment. CFU counts in aspirated TCF were measured at predetermined time points during the experiment and implanted materials were analyzed at the end of the follow-up. Planktonic bacterial counts in TCF increased by 1.62 Log_{10} CFU/mL over the 11-days period. All animals had positive cultures throughout the experiment (Fig. 10A). The average adherent bacterial count was 8.3 Log_{10} CFU per cage at day 11 (Fig. 10B).

3.8. Activity of antimicrobial treatments in vivo

3.8.1. Efficacy of treatments against planktonic and adherent bacteria

In the other groups of animals (C-D-E-F), local treatment was applied once (on day 3) while intraperitoneal vancomycin was administered twice daily over 4 days (days 3- to 6; Fig. 2). Bacterial counts in TCF (planktonic bacteria) or adhering on tissue cages or beads (biofilm) were monitored over time. Since all animals were administered the same intraperitoneal treatment, we compare the different groups based on the local treatment they received.

The planktonic bacterial count results are shown in Fig. 10A. Before treatment (day 3), CFU counts in TCF were similar in all groups (6.96 log_{10} CFU/mL in group C (P407), 6.95 log_{10} CFU/mL in group D (TEC in P407), 6.80 log_{10} CFU/mL in group E (VAN in P407) and 7.13 log_{10} in group F (VAN + TEC in P407), respectively). Twenty-four hours after the start of the treatment (day 4), we observed a significant reduction in CFU count in animals administered with local vancomycin alone (group E; 2.7 Log_{10} CFU/mL reduction) or combined with TEC (group F; 2.8 Log_{10} reduction), respectively. Only a 1.9 Log_{10} CFU/mL reduction was observed in animals having received local TEC only (group D) when compared to animals treated with local P407 only (group C) ($p < 0.001$). No regrowth was observed until the end of follow-up in groups E and F. In groups C and D, the CFU counts remained globally stable until the end of the experiment. Furthermore, the evolution of planktonic bacteria counts in groups C or D was comparable to that observed in untreated animals (Group B).

Adherent bacterial counts were assessed on explanted materials, after the animals were sacrificed (Fig. 10B). Twenty-four hours after the start of treatment (day 4), a significantly higher reduction in adherent bacterial counts was observed in animals treated with local VAN + TEC in P407 (group F) compared to animals treated with local vancomycin alone in P407 (group E; difference of 2.1 Log_{10}), local TEC alone in P407 (group D; difference of 2.3 Log_{10}) or local P407 without active agents

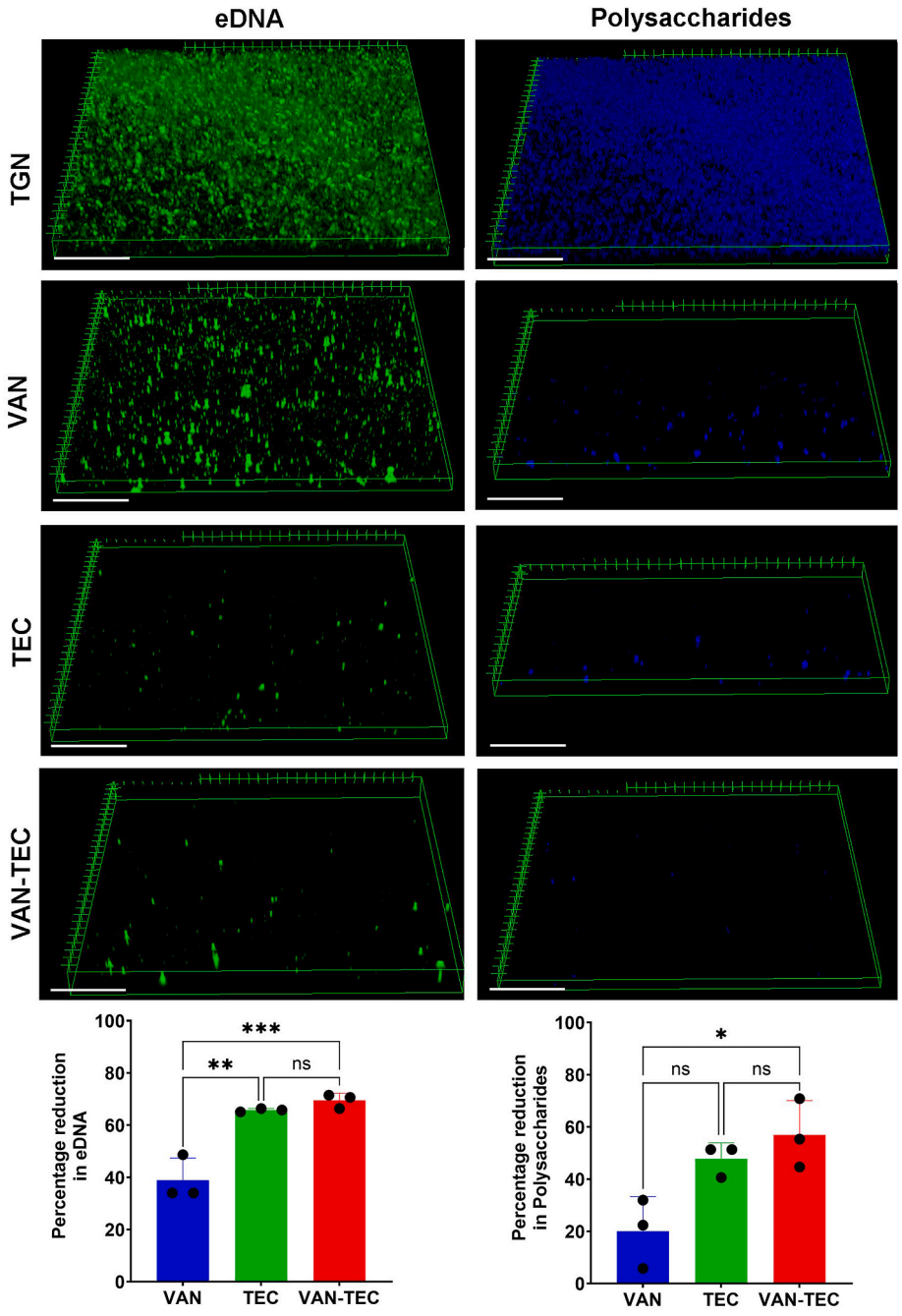

Fig. 7. Confocal microscopy images and quantitative analysis of extracellular matrix constituents. Extracellular DNA (eDNA, left) and extracellular polysaccharides (right) in mature MRSA ATCC33591 biofilms grown on titanium coupons and treated for 24 h with TGN (control), TEC, vancomycin 10 mg/mL (VAN), or their combination (VAN-TEC), all formulated in P407 hydrogel. Representative 3D-rendered maximum intensity projections of biofilm matrix components stained with TOTO-1 (eDNA, green) and Calcofluor White (EPS, blue). Images acquired at 40 × magnification, scale bars = 25 μm. Quantification of the % Area covered by eDNA and EPS for each condition based on average intensity projection of Z-stacks (n = 3–5 fields/condition). Percentage reduction in matrix components relative to the untreated control (TGN), calculated as: % Reduction= (1−(Mean signal treated/Mean signal TGN)) × 100. (For interpretation of the references to color in this figure legend, the reader is referred to the Web version of this article.)

(group C; difference of 4.3 Log_{10}). This difference remained significant at days 7 and 11 (i.e. after the end of the intraperitoneal treatment), although some regrowth was noticed at day 7 and 11 in animals treated with local TEC in P407 (group D; regain of 1.6 Log_{10} at day 11 compared to day 4) and local VAN + TEC in P407 (group F; regain of 1.8 Log_{10}).

3.9. Leucocytes count

Leucocytes counts are shown in Fig. 11. The baseline leucocyte counts were similar across the four groups and a uniform increase was observed following the inoculation. 24 h after the treatment period (day 7), we observed a significant decrease for animals from group E (VAN in P407) and F (VAN + TEC in P407) compared to animals from group C (P407; $p < 0.01$ and $p < 0.0001$, respectively). No significant difference was observed between animals in group D (TEC in P407) and in groups C (P407) or E (VAN in P407).

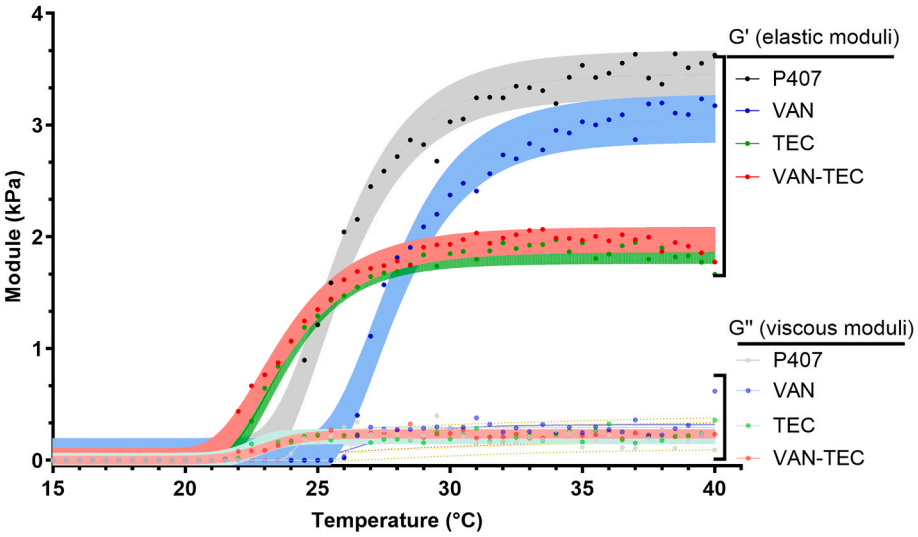

Table. Summary of key rheological parameters for P407-based formulations

Conditions	Tgel (°C)	G' plateau 35.5°C–38.5°C (kPa)	Slope ΔG'/ΔT (Pa/°C)
P407	24.5 ± 0.9	3.5 ± 0.46	166 ± 15
P407-VAN	26.5 ± 0.0 (ns)	3.1 ± 0.1 (ns)	151 ± 3*
P407-TEC	22.3 ± 0.3*	1.9 ± 0.8*	104 ± 2*
P407-VAN-TEC	22.0 ± 1.3*	2.0 ± 0.7*	97 ± 15*

Statistical analysis:

one-way ANOVA with Tukey HSD, comparing treatments versus P407 (*p<0.05)

Fig. 8. Rheological properties of poloxamer 407-based hydrogels with vancomycin (VAN, 10 mg/mL**), trienzymatic cocktail (TEC), or both (VAN-TEC).** Temperature-dependent evolution of viscoelastic moduli G′ (elastic modulus, solid lines) and G″ (viscous modulus, dotted lines) between 15 °C and 40 °C. The Table summarizes key rheological parameters including the sol-gel transition Tgel (°C), the plateau modulus (kPa), and gelation slope (Pa/°C). Data are shown as mean ± SD (n = 3). Statistical significance was assessed using one-way ANOVA with Dunnett's post hoc test, comparing treatments versus P407 (*p < 0.05). Rheological measurements were performed using a stress-controlled rotational rheometer (1 Hz, 0.1 % strain, 1 °C/min).

4. Discussion

The treatment of PJI, particularly those caused by MRSA, often requires prolonged antibiotic therapy and multiple revision surgeries [40]. To address this challenge, novel therapeutic approaches are being actively explored. A promising strategy to enhance the treatment of MRSA-associated implant infections involves the combined use of enzymatic cocktails and antibiotics [41], but this strategy has, to the best of our knowledge, not yet been evaluated *in vivo* in-depth.

In this study, we evaluate the potential of combining supratherapeutic doses of antibiotics with a tri-enzymatic cocktail (TEC) [15] incorporated in a thermosensitive poloxamer 407 hydrogel to enable their local delivery, retention and activity at the site of infection. Our findings demonstrate that the hydrogel formulation preserves the activity of both the antibiotics and enzymes, with efficacy *in vitro* comparable to that of the same agents delivered in solution. Additionally, we confirm that the combination of TEC with supratherapeutic vancomycin is more effective, resulting in significantly higher reduction in both CFU counts and biofilm biomass in an MRSA biofilms as compared to vancomycin or TEC alone [15]. Moreover, in an *in vivo* model of infection on implanted material, the local combination therapy with vancomycin and TEC, coupled to intraperitoneal vancomycin, was significantly more active against both planktonic and adherent bacteria than local monotherapies with vancomycin or TEC alone.

A key finding of the *in vitro* study was that the hydrogel formulation did not compromise the antibiofilm activity of the active agents on CFU counts and biomass, although antibiotics delivered via the hydrogel showed a slightly reduced efficacy (in general, not significantly) compared to their solution-based counterparts. This difference might be attributed to the immediate availability of active agents in solution, whereas hydrogels are designed for controlled release, which could delay the initial burst of antibiotic action [42]. Despite this limitation, hydrogels offer significant advantages over solutions, particularly in intra-articular applications, which are not evidencable *in vitro*. Unlike solutions, hydrogels minimize external loss of active agents following injection, ensuring their retention at high concentrations at the infection site and enabling localized and therapeutic effects while minimizing systemic exposure and toxicity [17,43].

The *in vitro* release kinetics of antibiotics and enzymes from the hydrogel reveals a biphasic profile—rapid and slow phases—consistent with the Higuchi model, indicative of controlled release [44]. Most of the active agents were liberated within the first 12 h, achieving high local concentrations essential for the early-stage biofilm treatment. Similar findings have been observed for drugs like tobramycin and daptomycin in poloxamer 407-based hydrogels [45]. Rapid release is advantageous for attaining high local concentrations at the onset of the treatment. Moreover, hydrophilic enzymes in TEC may alter the gel microenvironment at pH 7.4, increasing porosity and enhancing vancomycin diffusion.

The use of poloxamer 407 as a drug delivery vehicle offers additional

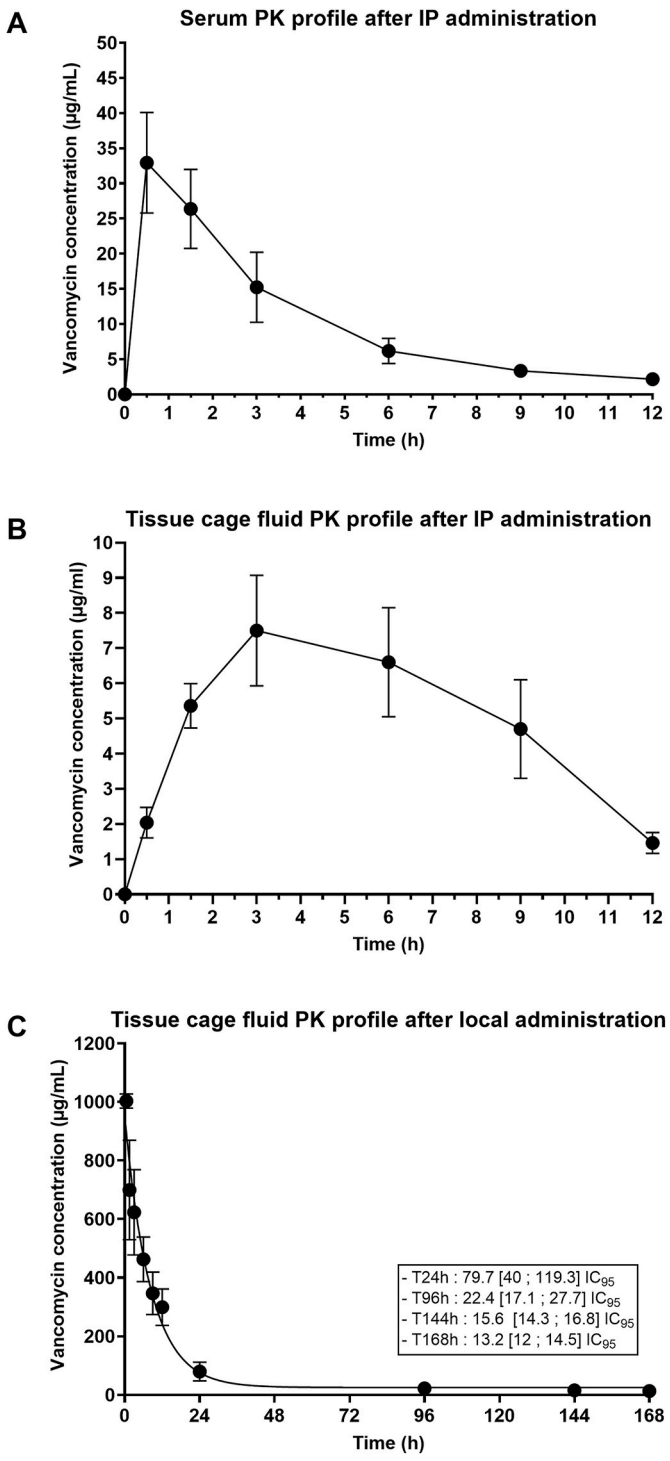

Fig. 9. Pharmacokinetic profile of vancomycin in serum (**A**) and tissue cage fluid (**B**) over time following administration of a single intraperitoneal dose of vancomycin at 15 mg/kg, or (**C**) in tissue cage fluid following local administration of P407 containing vancomycin at 10 mg/mL. Note differences in the Y-axis scale. Residual concentrations with their 95 % confidence interval are shown at specific time points in panel C. (A) N = 2, n = 3. (B and C) n = 5. Values are means ± SEM (A) or SD (B and C).

advantages for the *in vivo* delivery of active agents, particularly in the context of PJIs. Its thermosensitive properties allow it to remain fluid at low temperatures, facilitating ease of administration, and to gel at body temperature, enabling the controlled release of active agents [17,19]. *In vivo* pharmacokinetic data confirm the suitability of this formulation for controlled release, with local antibiotic concentrations remaining above the MIC for over seven days, with an $AUC_{0–168h}$ approximately 210-fold higher than systemic vancomycin. These findings are reassuring especially considering the slight modifications in the rheological properties of the gel caused by the incorporation of active agents. Of note, the mechanical stiffness of our formulation is in the same order of magnitude of that reported for poloxamer hydrogels loaded with small pharmacological agents like lidocaine [46], or proteins like recombinant tissue-type plasminogen activator [47]. Adequate pharmacokinetics are essential when designing injectable delivery systems for clinical application, particularly for localized treatment of infections where timing and mechanical performance are critical.

In vitro, the vancomycin-TEC combination delivered via hydrogel achieved a significantly higher reduction in CFU counts and biomass compared to monotherapies, demonstrating a marked improvement in efficacy. Vancomycin often shows limited activity against biofilms due to its poor penetration across the protective extracellular matrix [48]. TEC degrades key structural components of this matrix—such as extracellular DNA/RNA [49], cellulose [50], and Poly--β-(1–6)-*N*-acetylglucosamine [51]— as clearly confirmed here by confocal microscopy imaging of matrix constituents. This matrix-disrupting effect compromises biofilm integrity, facilitating antibiotic access to embedded bacteria. Notably, TEC alone is ineffective against viable bacteria, highlighting the importance of combination with antibiotic therapy. Our previous work demonstrated the efficacy of a similar tri-enzymatic cocktail combined with therapeutic-dose antibiotics against staphylococcal biofilms [15]. Here, we extend these findings by showing that TEC maintains its efficacy even when combined with supratherapeutic antibiotic concentrations suitable for local co-administration, reinforcing its potential as a potent adjunct in treating biofilm-associated infections. Importantly also, we did not observe any reduction in the activity of the TEC over the global time course of our whole set experiments, confirming the stability established by its manufacturer. This stability will however need to be confirmed by specific testing following the ad hoc procedures established for the preclinical development for medical products.

When combined with fluoroquinolones, TEC does not show strong synergistic effects, likely due to the inherent ability of fluoroquinolones to penetrate effectively the biofilm matrix owing their small molecular size and moderate hydrophobicity [52,53]. Known for its broad-spectrum activity, including against MRSA [54], moxifloxacin is particularly well-suited for targeting biofilm-associated *S. aureus*, while ciprofloxacin is occasionally used empirically due to its broad-spectrum coverage and favorable pharmacokinetics [24]. In this study, moxifloxacin confirms its superior antibiofilm efficacy, reducing both CFU counts and biofilm biomass whether delivered in solution or via hydrogel, even at lower multiples of its MIC. Incorporation in hydrogel could further enhance moxifloxacin retention and delivery within biofilms *in vivo*, although this benefit is not visible in our *in vitro* setting where therapeutic agents remain in contact with the biofilm throughout the experiment [55]. However, the use of fluoroquinolones at high local concentrations warrants caution due to potential adverse effects such as tendonitis and tendon rupture [56], reinforcing the rationale to prioritize the evaluation of the TEC-vancomycin hydrogel *in vivo*.

In vivo, intraperitoneal vancomycin combined with local P407 without active agents (group C) led to minimal reduction in bacterial counts compared to the untreated group B, confirming that the hydrogel itself lacks antimicrobial properties, consistent with *in vitro* findings. Local administration of vancomycin (group E) significantly enhanced the efficacy of the intraperitoneal treatment against planktonic MRSA, achieving a rapid and sustained reduction in bacterial counts, with maximal efficacy 24 h post-treatment, outperforming both the local TEC in P407 (group D) or P407 without active agents (group C). Notably, we employed supratherapeutic doses of vancomycin locally, to maintain therapeutic levels at the infection site over the long term while minimizing the risk of toxicity associated with high serum levels. Systemic

Table 3
Pharmacokinetic parameters of vancomycin in guinea pig serum after intraperitoneal (ip)administration. N = 2, n = 3 (serum) or n = 5 (tissue cage fluid). Values are means ± SEMs (serum) or SD (tissue cage fluid).

Vancomycin dose	Route of administration	Site of sampling	Parameters				
			C_{max} (μg/mL)	C_{min} (12 h) (μg/mL)	AUC $_{0–12h}$ (μg.h/mL)	$T_{1/2}$ (h)	T_{max} (h)
15 mg/kg	IP	Serum	32.95 (±5.8)	2.16 (±0.4)	123.8 (±6.6)	2.82	0.5
		TCF	7.5 (±1.6)	1.46 (±0.3)	61.2 (±5.2)	13.7	3

Table 4
Pharmacokinetic parameters of vancomycin in tissue cage fluid after a single injection of P407 formulation containing 10 mg/mL of vancomycin. n = 5 (tissue cage fluid). Values are means±SD.

Vancomycin dose	Route of administration	Site of sampling	Parameters					
			C_{max} (μg/mL)	C_{min} (168 h) (μg/mL)	AUC $_{0–168h}$ (μg.h/mL)	$T_{1/2}$ (h)	T_{max} (h)	K (h^{-1})
10 mg/mL	Local	TCF	1000 (±24.1)	13.23 (±1.02)	12,862 (±1293)	5.7	0	0.12 (±0.03)

vancomycin alone failed to reach the pharmacodynamic target of $AUC_{0–24h}$/MIC >350 [57] for *S. aureus* infections, in both the serum and the TCF, with the C_{max} in TCF only 7-fold higher than the MIC (1 mg/L), a value comparable to that reported in the study Widmer et al. [58]. In contrast, local administration of vancomycin (10 mg/mL in hydrogel) exceeded this target, achieving an AUC_0-∞/MIC ratio >12,000, proportionally comparable to that observed by Veyries et al. at 40 mg/mL [16]. Thus, local administration sustains therapeutic vancomycin concenrations at the infection site without elevating systemic levels, maintaining extended exposure at the infection site while systemic administration leads to rapid drug clearance.

Combining local TEC with intraperitoneal vancomycin (group F) did not enhance clearance of planktonic bacteria but significantly reduced adherent bacterial populations. This confirms that enzymatic therapy does not exert direct antimicrobial action against free-floating bacteria [15,59,60] but facilitates antibiotic activity in biofilms. This finding corroborates our previous *in vitro* observations [15]. However, the treatment produced only transient effects on adherent bacteria, emphasizing its insufficiency as a standalone therapy and the need for combination strategies to achieve sustained bacterial clearance. The enhanced effect was indeed more pronounced when intraperitoneal vancomycin was combined with the local administration of both a high concentration of vancomycin and TEC, resulting in a sustained reduction in both non-adherent and adherent bacterial populations.

It is worth mentioning that we did not include a group treated exclusively with the combination hydrogel (vancomycin + TEC) in the absence of systemic vancomycin. This decision was justified by ethical considerations, in the line of the 3R rule and EU Directive 2010/63 [61], which recommend avoiding leaving infected animals without systemic antimicrobial therapy. In the group receiving intraperitoneal vancomycin combined with a blank hydrogel (P407 alone), bacterial loads remained high, indicating that systemic treatment alone had limited impact, if any. Conversely, our observations suggest that local treatment alone would likely be insufficient to eradicate the infection. Our pharmacokinetic data show that serum vancomycin concentrations were undetectable after local administration, exposing animals to a high risk of spreading of the infection in the absence of systemic coverage. Lastly, our study was designed to mimic clinical conditions, where local delivery systems are systematically combined with systemic antibiotics. Our model thus aimed to assess whether local adjuvant therapy can enhance systemic efficacy, rather than replace it.

Importantly, no signs of local intolerance were observed in guinea pigs, which was expected, as the enzymes in TEC primarily target biofilm components that are absent from human cells. This enhanced effect offers a strategic advantage in targeting biofilm-protected bacteria, which are notoriously resilient to conventional monotherapies [62], even at high local concentrations. A few *in vivo* studies have explored enzyme-based matrix disruption to enhance antimicrobial agent activity against biofilm infections. For example, in a pig skin model, extracellular polymeric substance (EPS)-degrading enzymes (dispersin B and DNase I) effectively detached adherent *S. aureus* and *S. epidermidis*, increasing susceptibility to antiseptics [63]. Similarly, proteolytic enzymes (serratiopeptidase) enhanced antibiotic activity in an implant-related *S. epidermidis* infection model [64].

Despite these promising results, certain limitations of this study should be acknowledged. First, we used a single MRSA strain, which limits the generalizability of findings to other strains or clinically relevant pathogens. Biofilm-forming bacteria such as *S. epidermidis* or *Pseudomonas aeruginosa* —also common in PJIs [8]— may respond differently to this combination therapy. However, the broad spectrum of the TEC cocktail has been demonstrated *in vitro* [15]. Similarly, using clinical isolates instead of a reference strain could enhance the relevance of findings, as different strains exhibit varying biofilm-forming capacities. Yet, reference strains facilitate reproducibility in *in vivo* studies. The MRSA strain used in this study is well-characterized, lacks the *Panton-Valentine Leukocidin* gene (resulting in reduced virulence), and has been extensively used in our previous biofilm studies [33,65]. Second, we administered a single antibiotic via intraperitoneal injection, while PJI treatment typically involves antibiotic combinations [66]. Our objective was to demonstrate improved efficacy of TEC when combined with vancomycin, a first-choice MRSA antibiotic which has moderate efficacy. Additionally, the short treatment period was due to guinea pig intolerance to prolonged antibiotic exposure, which can lead to antibiotic-associated enterotoxemia given their predominantly Gram-positive gut microbiota [67]. Third, while no signs of local intolerance were observed in guinea pigs, a potential immunogenic response to the enzymatic cocktail was not evaluated in this study. This is an important consideration for future research. Lastly, the observed bacterial regrowth at the end of follow-up underscores the resilience of biofilm-associated infections [68] and the challenge of achieving complete eradication. Contributing factors may include persister cells [69], incomplete biofilm disruption [70], and bacterial adaptive responses [71], suggesting that prolonged or repeated therapy may be necessary to prevent relapse.

5. Conclusion

The combination of vancomycin and a tri-enzymatic cocktail formulated in a thermosensitive poloxamer 407 hydrogel demonstrates significant potential for treating biofilm-associated infections on implanted material, particularly in reducing adherent MRSA counts. This high efficacy is attributable to the slow and sustained release of high antibiotic concentrations combined with to the disrupting effect of enzymes on the biomass matrix. The interest of the combination is particularly evident for antimicrobials whose efficacy is limited by poor matrix permeability. These findings underscore the potential of this

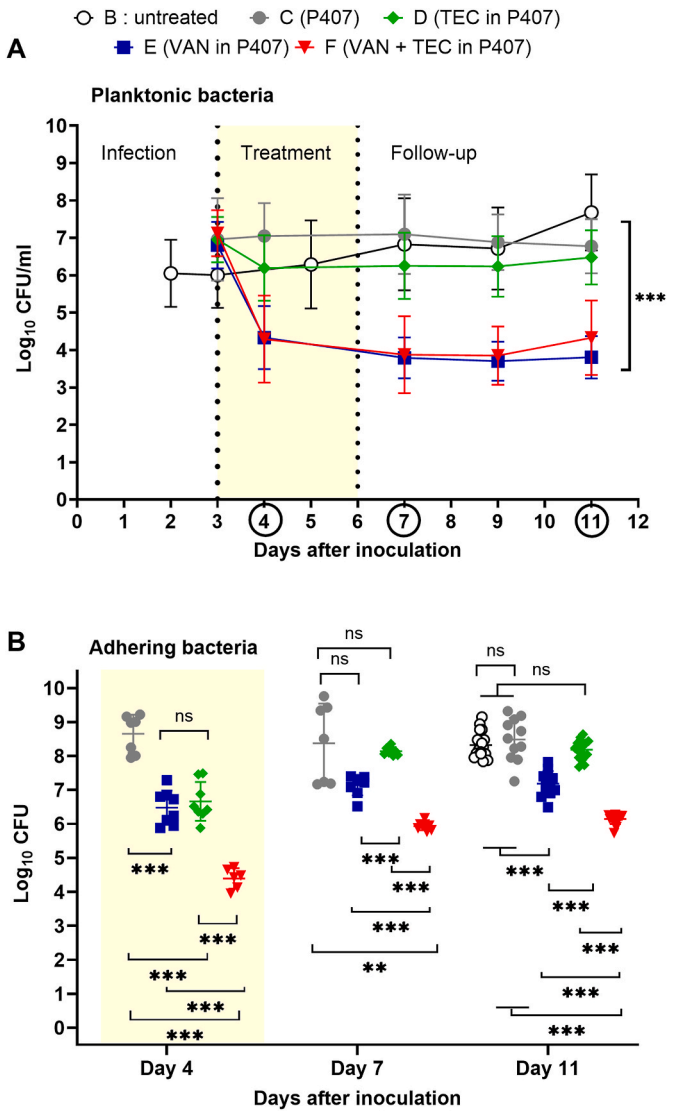

Fig. 10. Evolution of planktonic bacteria in tissue cage fluid (A) and of bacteria adhering to the implanted material (B) overtime. At 2 weeks after implantation, MRSA ATCC33591 (10^7 CFU) was inoculated into tissue cages (day 0). Animals from group B were left untreated and the number of CFU was determined in aspirated cage fluid at preset time points until the end of follow-up or on implanted material at day 11 after sacrifice (n = 18 from 5 animals). Animals from the other groups received a single local injection of 1-mL of P407 (group C) or P407 containing either TEC (group D) or vancomycin at 10 mg/mL (group E) or their combination (group F), followed by vancomycin at 15 mg/kg *ip* (twice daily for 4 days, indicated by the yellow area [days 3–6]. The number of CFU in aspirated cage fluid was determined at day 3, 4, 7, 9 and 11 and on material, in animals sacrificed at specified intervals, circled in panel A (day 4; 24h after starting the treatment): n = 7–8 from 2 animals; day 7; 24 h after the end of the treatment: n = 7–8 from 2 animals; day 11; end of follow up: n = 12–16 from 4 animals). Results are presented as means ± SD. Statistical analysis, two-way ANOVA followed by Tukey HSD multiple comparison. ns: not significant, **: $p < 0.01$; ***: $p < 0.001$. (For interpretation of the references to color in this figure legend, the reader is referred to the Web version of this article.)

approach for managing biofilm-associated infections, warranting further optimization to confirm its clinical applicability.

CRediT authorship contribution statement

Randy Buzisa Mbuku: Writing – original draft, Methodology, Investigation, Formal analysis, Conceptualization. **Hervé Poilvache:**

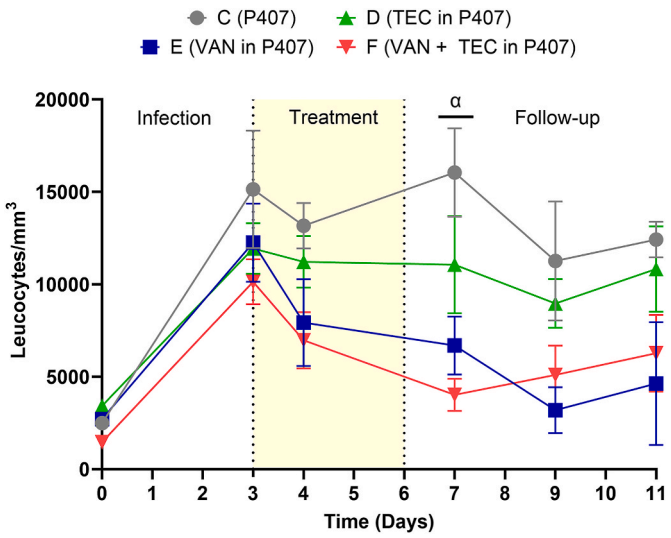

Fig. 11. Evolution of the total leukocytes counts in tissue cage fluid. At 2 weeks after implantation, MRSA ATCC33591 (10^7 CFU) was inoculated into tissue cages (day 0), and subsequently tissue cage fluid was aspirated at preset time points, from treatment until the end of follow-up. Results are presented as means ± SD. Statistical analysis, two-way ANOVA followed by Tukey HSD multiple comparison. α: statistically significant difference between groups C and D, and C and F.

Writing – review & editing, Conceptualization. **Loïc Maigret:** Writing – review & editing, Investigation. **Rita Vanbever:** Formal analysis, Methodology, Writing – review & editing. **Françoise Van Bambeke:** Writing – review & editing, Supervision, Funding acquisition, Formal analysis, Conceptualization. **Olivier Cornu:** Writing – review & editing, Supervision, Funding acquisition, Formal analysis, Conceptualization.

Declaration of generative AI in scientific writing

During the preparation of this work the author(s) used ChatGPT in order to improve readability and language. After using this tool, the author(s) reviewed and edited the content as needed and take(s) full responsibility for the content of the publication.

Declaration of competing interest

The authors declare the following financial interests/personal relationships which may be considered as potential competing interests:

Francoise Van Bambeke reports financial support was provided by Fund for Scientific Research. Francoise Van Bambeke reports financial support was provided by Walloon Region. Randy Busiza Mbuku reports financial support was provided by Fund for Research and Training in Industry and Agriculture. Olivier Cornu reports financial support was provided by Walloon Region. Francoise Van Bambeke and Olivier Cornu reports a relationship with Onelife SA that includes: funding grants. If there are other authors, they declare that they have no known competing financial interests or personal relationships that could have appeared to influence the work reported in this paper.

Acknowledgements

We thank Alix Mangin for his expert technical help and Prof. Anne des Rieux (Louvain Drug Research Institute) for advice regarding the formulation of the hydrogel. We are also grateful to Dr Caroline Bouzin (2IP imaging platform, IREC, UCLouvain) for her support with confocal image processing and to Lidvine Boland (LTAP, IREC and cliniques universitaires Saint-Luc, UCLlouvain) for help in vancomycin assays. We thank OneLife SA for providing the trienzymatic cocktail for academic

research purposes and to its R&D team for scientific advice. The work was funded by the Win2Wal program of the Region Wallonne (Orthenzy project) and by the Belgian FRS-FNRS (grant J.0177.23). RBM is the beneficiary of a FRIA (Fonds pour la formation à la Recherche dans l'Industrie et dans l'Agriculture) grant of the FRS-FNRS (ID: 40021965). FVB is a research director of the FRS-FNRS.

Appendix A. Supplementary data

Supplementary data to this article can be found online at https://doi.org/10.1016/j.bioflm.2025.100288.

Data availability

Data will be made available on request.

References

[1] Bernthal NM, Park HY, Zoller SD, Petrigliano FA. Implant engineering in the age of biologics. J Am Acad Orthop Surg 2019;27:e685–90. https://doi.org/10.5435/JAAOS-D-17-00503.
[2] Korolyov AY. Metal-based implants: review of materials and designs. Sci Tech 2024;23:204–18. https://doi.org/10.21122/2227-1031-2024-23-3-204-218.
[3] Jiao J, Zhang S, Qu X, Yue B. Recent advances in research on antibacterial metals and alloys as implant materials. Front Cell Infect Microbiol 2021;11:693939. https://doi.org/10.3389/fcimb.2021.693939.
[4] Xu Y, Huang TB, Schuetz MA, Choong PFM. Mortality, patient-reported outcome measures, and the health economic burden of prosthetic joint infection. EFORT Open Rev 2023;8(9):690–7. https://doi.org/10.1530/eor-23-0078.
[5] Premkumar A, Kolin DA, Farley KX, Wilson JM, McLawhorn AS, Cross MB, et al. Projected economic burden of periprosthetic joint infection of the hip and knee in the United States. J Arthroplast 2021;36(5):1484. https://doi.org/10.1016/j.arth.2020.12.005. 9.e3.
[6] Arciola CR, Campoccia D, Montanaro L. Implant infections: adhesion, biofilm formation and immune evasion. Nat Rev Microbiol 2018;16:397–409. https://doi.org/10.1038/s41579-018-0019-y.
[7] Fux CA, Costerton JW, Stewart PS, Stoodley P. Survival strategies of infectious biofilms. Trends Microbiol 2005;13(1):34–40. https://doi.org/10.1016/j.tim.2004.11.010.
[8] Aggarwal VK, Bakhshi H, Ecker NU, Parvizi J, Gehrke T, Kendoff D. Organism profile in periprosthetic joint infection: pathogens differ at two arthroplasty infection referral centers in Europe and in the United States. J Knee Surg 2014;27(5):399–406. https://doi.org/10.1055/s-0033-1364102.
[9] An YH, Friedman RJ. Prevention of sepsis in total joint arthroplasty. J Hosp Infect 1996;33(2):93–108. https://doi.org/10.1016/s0195-6701(96)90094-8.
[10] Gonzalez MR, Pretell-Mazzini J, Lozano-Calderon SA. Risk factors and management of prosthetic joint infections in megaprostheses—a review of the literature. Antibiotics 2024;13(1):25. https://doi.org/10.3390/antibiotics13010025.
[11] Dzaja I, Howard J, Somerville L, Lanting B. Functional outcomes of acutely infected knee arthroplasty: a comparison of different surgical treatment options. Can J Surg 2015;58(6):402–7. https://doi.org/10.1503/cjs.017614.
[12] Urish KL, Bullock AG, Kreger AM, Shah NB, Jeong K, Rothenberger SD. A multicenter study of irrigation and debridement in total knee arthroplasty periprosthetic joint infection: treatment failure is high. J Arthroplast 2018;33(4):1154–9. https://doi.org/10.1016/j.arth.2017.11.029.
[13] Steadman W, Chapman PR, Schuetz M, Schmutz B, Trampuz A, Tetsworth K. Local antibiotic delivery options in prosthetic joint infection. Antibiotics (Basel) 2023;12(4):752. https://doi.org/10.3390/antibiotics12040752.
[14] Aparicio-Blanco J, Lopez T, Alonso-Berenguel M, Torres-Suarez AI, Martin-Sabroso C. Local antimicrobial delivery systems for prophylaxis and treatment of periprosthetic traumatological infections. Eur J Pharmaceut Sci 2025;204:106940. https://doi.org/10.1016/j.ejps.2024.106940.
[15] Poilvache H, Ruiz-Sorribas A, Cornu O, Van Bambeke F. In-vitro study of the synergistic effect of an enzyme cocktail and antibiotics against biofilms in a prosthetic joint infection model. Antimicrob Agents Chemother 2021;65(4):e01699. https://doi.org/10.1128/AAC.01699-20. 20.
[16] Veyries ML, Couarraze G, Geiger S, Agnely F, Massias L, Kunzli B, et al. Controlled release of vancomycin from poloxamer 407 gels. Int J Pharm 1999;192(2):183–93. https://doi.org/10.1016/s0378-5173(99)00307-5.
[17] Dumortier G, Grossiord JL, Agnely F, Chaumeil JC. A review of poloxamer 407 pharmaceutical and pharmacological characteristics. Pharm Res 2006;23(12):2709–28. https://doi.org/10.1007/s11095-006-9104-4.
[18] Russo E, Villa C. Poloxamer hydrogels for biomedical applications. Pharmaceutics 2019;11(12):671. https://doi.org/10.3390/pharmaceutics11120671.
[19] Fakhari A, Corcoran M, Schwarz A. Thermogelling properties of purified poloxamer 407. Heliyon 2017;3(8):e00390. https://doi.org/10.1016/j.heliyon.2017.e00390.
[20] Lade H, Park JH, Chung SH, Kim IH, Kim JM, Joo HS, et al. Biofilm Formation by Staphylococcus aureus clinical isolates is differentially affected by glucose and sodium chloride supplemented culture media. J Clin Med 2019;8(11):1853. https://doi.org/10.3390/jcm8111853.
[21] Liu M, Blinn C, McLeod SM, Wiseman JW, Newman JV, Fisher SL, et al. Secreted Gaussia princeps luciferase as a reporter of Escherichia coli replication in a mouse tissue cage model of infection. PLoS One 2014;9(3):e90382. https://doi.org/10.1371/journal.pone.0090382.
[22] Rybak M, Lomaestro B, Rotschafer JC, Moellering Jr R, Craig W, Billeter M, et al. Therapeutic monitoring of vancomycin in adult patients: a consensus review of the American society of health-system pharmacists, the infectious diseases society of America, and the society of infectious diseases pharmacists. Am J Health Syst Pharm 2009;66(1):82–98. https://doi.org/10.2146/ajhp080434.
[23] Juan S, Garcia-Reyne A, Caba P, Chaves F, Resines C, Llanos F, et al. Safety and efficacy of moxifloxacin monotherapy for treatment of orthopedic implant-related staphylococcal infections. Antimicrob Agents Chemother 2010;54:5161–6. https://doi.org/10.1128/AAC.00027-10.
[24] Zahr N, Urien S, Aubry A, Chauvin C, Comets E, Llopis B, et al. Ciprofloxacin population pharmacokinetics during long-term treatment of osteoarticular infections. J Antimicrob Chemother 2021;76:2906–13. https://doi.org/10.1093/jac/dkab275.
[25] Sun S, Wang Q, Zhang B, Cui Y, Si X, Wang G, et al. Vancomycin-loaded in situ gelled hydrogel as an antibacterial system for enhancing repair of infected bone defects. Int J Nanomed 2024;19:10227–45. https://doi.org/10.2147/ijn.S448876.
[26] Zou C, Guo W, Mu W, Wahafu T, Li YHL, Xu B, et al. Synovial vancomycin and meropenem concentrations in periprosthetic joint infection treated by single-stage revision combined with intra-articular infusion. Bone Joint Res 2024;13(10):535–45. https://doi.org/10.1302/2046-3758.1310.Bjr-2024-0024.R2.
[27] Ruiz-Sorribas A, Poilvache H, Kamarudin NHN, Braem A, Van Bambeke F. Hydrolytic enzymes as potentiators of antimicrobials against an inter-kingdom biofilm model. Microbiol Spectr 2022;10(1):e0258921. https://doi.org/10.1128/spectrum.02589-21.
[28] Schmolka IR. Artificial skin. I. Preparation and properties of pluronic F-127 gels for treatment of burns. J Biomed Mater Res 1972;6(6):571–82. https://doi.org/10.1002/jbm.820060609.
[29] Russo E, Villa C. Poloxamer hydrogels for biomedical applications. Pharmaceutics 2019;11(12). https://doi.org/10.3390/pharmaceutics11120671.
[30] Geneva II, Cuzzo B, Fazili T, Javaid W. Normal body temperature: a systematic review. Open Forum Infect Dis 2019;6. https://doi.org/10.1093/ofid/ofz032.
[31] The European Committee on Antimicrobial Susceptibility Testing. Breakpoint tables for interpretation of MICs and zone diameters, Version 14.0; 2024. http://www.eucast.org.
[32] Michot JM, Seral C, Van Bambeke F, Mingeot-Leclercq MP, Tulkens PM. Influence of efflux transporters on the accumulation and efflux of four quinolones (ciprofloxacin, levofloxacin, garenoxacin, and moxifloxacin) in J774 macrophages. Antimicrob Agents Chemother 2005;49(6):2429–37. https://doi.org/10.1128/aac.49.6.2429-2437.2005.
[33] Poilvache H, Ruiz-Sorribas A, Sakoulas G, Rodriguez-Villalobos H, Cornu O, Van Bambeke F. Synergistic effects of pulsed lavage and antimicrobial therapy against Staphylococcus aureus biofilms in an in-vitro model. Front Med (Lausanne) 2020;7:527. https://doi.org/10.3389/fmed.2020.00527.
[34] Schindelin J, Arganda-Carreras I, Frise E, Kaynig V, Longair M, Pietzsch T, et al. Fiji: an open-source platform for biological-image analysis. Nat Methods 2012;9(7):676–82. https://doi.org/10.1038/nmeth.2019.
[35] Otsu N. A threshold selection method from gray-level histograms. IEEE Trans Syst Man Cybern Syst Hum 1979;9(1):62–6. https://doi.org/10.1109/TSMC.1979.4310076.
[36] Wang Z, Vanbever R, Lorent JH, Solis J, Knoop C, Van Bambeke F. Repurposing DNase I and alginate lyase to degrade the biofilm matrix of dual-species biofilms of Staphylococcus aureus and Pseudomonas aeruginosa grown in artificial sputum medium: in-vitro assessment of their activity in combination with broad-spectrum antibiotics. J Cyst Fibros 2024;23(6):1146–52. https://doi.org/10.1016/j.jcf.2024.02.012.
[37] Zimmerli W, Waldvogel FA, Vaudaux P, Nydegger UE. Pathogenesis of foreign body infection: description and characteristics of an animal model. J Infect Dis 1982;146(4):487–97. https://doi.org/10.1093/infdis/146.4.487.
[38] Ellen YC, Flecknell PA, Leach MC. Evaluation of using behavioural changes to assess post-operative pain in the Guinea pig (Cavia porcellus). PLoS One 2016;11:e0161941. https://doi.org/10.1371/journal.pone.0161941.
[39] Slinker BK. The statistics of synergism. J Mol Cell Cardiol 1998;30(4):723–31. https://doi.org/10.1006/jmcc.1998.0655.
[40] Lora-Tamayo J, Murillo O, Iribarren JA, Soriano A, Sanchez-Somolinos M, Baraia-Etxaburu JM, et al. A large multicenter study of methicillin-susceptible and methicillin-resistant Staphylococcus aureus prosthetic joint infections managed with implant retention. Clin Infect Dis 2013;56(2):182–94. https://doi.org/10.1093/cid/cis746.
[41] Hogan S, Zapotoczna M, Stevens NT, Humphreys H, O'Gara JP, O'Neill E. Potential use of targeted enzymatic agents in the treatment of Staphylococcus aureus biofilm-related infections. J Hosp Infect 2017;96(2):177–82. https://doi.org/10.1016/j.jhin.2017.02.008.
[42] Gallastegui A, Spesia MB, dell'Erba IE, Chesta CA, Previtali CM, Palacios RE, et al. Controlled release of antibiotics from photopolymerized hydrogels: kinetics and microbiological studies. Mater Sci Eng C 2019;102:896–905. https://doi.org/10.1016/j.msec.2019.04.027.
[43] Kildow BJ, Patel SP, Otero EJ, Fehring KA, Curtin BM, Springer BD, et al. Results of debridement, antibiotics, and implant retention for periprosthetic knee joint infection supplemented with the use of intraosseous antibiotics. Bone Joint Lett J

2021;103-B(6 Supple A):185–90. https://doi.org/10.1302/0301-620x.103b6.Bjj-2020-2278.R1.
[44] Akkari ACS, Papini JZB, Garcia GK, Franco M, Cavalcanti LP, Gasperini A, et al. Poloxamer 407/188 binary thermosensitive hydrogels as delivery systems for infiltrative local anesthesia: physico-chemical characterization and pharmacological evaluation. Mater Sci Eng C Mater Biol Appl. 2016;68:299–307. https://doi.org/10.1016/j.msec.2016.05.088.
[45] Lane DD, Fessler AK, Goo S, Williams DL, Stewart RJ. Sustained tobramycin release from polyphosphate double network hydrogels. Acta Biomater 2017;50:484–92. https://doi.org/10.1016/j.actbio.2016.12.030.
[46] Ricci EJ, Bentley MV, Farah M, Bretas RE, Marchetti JM. Rheological characterization of Poloxamer 407 lidocaine hydrochloride gels. Eur J Pharmaceut Sci 2002;17(3):161–7. https://doi.org/10.1016/s0928-0987(02)00166-5.
[47] Thiebaut AM, Louet ER, Ianszen M, Guichard MJ, Hanley DF, Gaudin C, et al. O2L-001, an innovative thrombolytic to evacuate intracerebral haematoma. Brain 2023;146(11):4690–701. https://doi.org/10.1093/brain/awad237.
[48] Jefferson KK, Goldmann DA, Pier GB. Use of confocal microscopy to analyze the rate of vancomycin penetration through Staphylococcus aureus biofilms. Antimicrob Agents Chemother 2005;49(6):2467–73. https://doi.org/10.1128/aac.49.6.2467-2473.2005.
[49] Nestle M, Roberts WK. An Extracellular Nuclease from Serratia marcescens: I. Purification and some properties of the enzyme. J Biol Chem 1969;244(19):5213–8. https://doi.org/10.1016/S0021-9258(18)63648-8.
[50] Zogaj X, Bokranz W, Nimtz M, Römling U. Production of cellulose and curli fimbriae by members of the family Enterobacteriaceae isolated from the human gastrointestinal tract. Infect Immun 2003;71(7):4151–8. https://doi.org/10.1128/iai.71.7.4151-4158.2003.
[51] Kaplan JB, Ragunath C, Ramasubbu N, Fine Daniel H. Detachment of Actinobacillus actinomycetemcomitans biofilm cells by an endogenous β-hexosaminidase activity. J Bacteriol 2003;185(16):4693–8. https://doi.org/10.1128/jb.185.16.4693-4698.2003.
[52] Singh R, Ray P, Das A, Sharma M. Penetration of antibiotics through Staphylococcus aureus and Staphylococcus epidermidis biofilms. J Antimicrob Chemother 2010;65(9):1955–8. https://doi.org/10.1093/jac/dkq257.
[53] Geremia N, Giovagnorio F, Colpani A, De Vito A, Botan A, Stroffolini G, et al. Fluoroquinolones and biofilm: a narrative review. Pharmaceuticals 2024;17(12):1673. https://doi.org/10.3390/ph17121673.
[54] Galani L, Pefanis A, Sakka V, Iliopoulos D, Donta I, Triantafyllidi H, et al. Successful treatment with moxifloxacin of experimental aortic valve endocarditis due to methicillin-resistant Staphylococcus aureus (MRSA). Int J Antimicrob Ag 2009;33(1):65–9. https://doi.org/10.1016/j.ijantimicag.2008.07.021.
[55] Shastri DH, Prajapati ST, Patel LD. Design and development of thermoreversible ophthalmic in situ hydrogel of moxifloxacin HCl. Curr Drug Deliv 2010;7(3):238–43. https://doi.org/10.2174/156720110791560928.
[56] Shu Y, Zhang Q, He X, Liu Y, Wu P, Chen L. Fluoroquinolone-associated suspected tendonitis and tendon rupture: a pharmacovigilance analysis from 2016 to 2021 based on the FAERS database. Front Pharmacol 2022;13(13):990241. https://doi.org/10.3389/fphar.2022.990241.
[57] European committee on antimicrobial susceptibility testing (EUCAST). Vancomycin: rationale for the EUCAST clinical breakpoints. 2010. version 2.1 Växjö, Sweden (EUCAST). Technical report. Available from, https://www.eucast.org/fileadmin/src/media/PDFs/EUCAST_files/Rationale_documents/Vancomycin_rationale_2.1.pdf.
[58] Widmer AF, Frei R, Rajacic Z, Zimmerli W. Correlation between in vivo and in vitro efficacy of antimicrobial agents against foreign body infections. J Infect Dis 1990;162(1):96–102. https://doi.org/10.1093/infdis/162.1.96.
[59] Kaplan JB, Ragunath C, Velliyagounder K, Fine DH, Ramasubbu N. Enzymatic detachment of Staphylococcus epidermidis biofilms. Antimicrob Agents Chemother 2004;48(7):2633–6. https://doi.org/10.1128/AAC.48.7.2633-2636.2004.
[60] Fleming D, Rumbaugh KP. Approaches to dispersing medical biofilms. Microorganisms 2017;5(2):15. https://doi.org/10.3390/microorganisms5020015.
[61] Ali O. A brief review of the European directive on 3Rs and facilitating animal experimentation. Acta Agraria Kaposváriensis 2023;27:7–28. https://doi.org/10.31914/aak.4191.
[62] Stewart PS, Costerton JW. Antibiotic resistance of bacteria in biofilms. Lancet 2001;358(9276):135–8. https://doi.org/10.1016/s0140-6736(01)05321-1.
[63] Kaplan JB, Mlynek KD, Hettiarachchi H, Alamneh YA, Biggemann L, Zurawski DV, et al. Extracellular polymeric substance (EPS)-degrading enzymes reduce staphylococcal surface attachment and biocide resistance on pig skin in vivo. PLoS One 2018;13(10):e0205526. https://doi.org/10.1371/journal.pone.0205526.
[64] Mecikoglu M, Saygi B, Yildirim Y, Karadag-Saygi E, Ramadan SS, Esemenli T. The effect of proteolytic enzyme serratiopeptidase in the treatment of experimental implant-related infection. J Bone Joint Surg Am 2006;88(6):1208–14. https://doi.org/10.2106/jbjs.E.00007.
[65] Poilvache H, Van Bambeke F, Cornu O. Development of an innovative in vivo model of PJI treated with DAIR. Front Med (Lausanne) 2022;9:984814. https://doi.org/10.3389/fmed.2022.984814.
[66] Tande AJ, Patel R. Prosthetic joint infection. Clin Microbiol Rev 2014;27(2):302–45. https://doi.org/10.1128/CMR.00111-13.
[67] O'Rourke DP. Disease problems of Guinea pigs. Ferrets, Rabbits, and Rodents 2004:245–54. https://doi.org/10.1016/B0-72-169377-6/50026-5.
[68] Yan J, Bassler BL. Surviving as a community: antibiotic tolerance and persistence in bacterial biofilms. Cell Host Microbe 2019;26(1):15–21. https://doi.org/10.1016/j.chom.2019.06.002.
[69] Fisher RA, Gollan B, Helaine S. Persistent bacterial infections and persister cells. Nat Rev Microbiol 2017;15(8):453–64. https://doi.org/10.1038/nrmicro.2017.42.
[70] Han Q, Jiang Y, Brandt BW, Yang J, Chen Y, Buijs MJ, et al. Regrowth of microcosm biofilms on titanium surfaces after various antimicrobial treatments. Front Microbiol 2019;10:2693. https://doi.org/10.3389/fmicb.2019.02693.
[71] Uruén C, Chopo-Escuin G, Tommassen J, Mainar-Jaime RC, Arenas J. Biofilms as promoters of bacterial antibiotic resistance and tolerance. Antibiotics 2020;10(1):3. https://doi.org/10.3390/antibiotics10010003.

Targeting *Staphylococcus aureus* biofilm-related infections on implanted material with a novel dual-action thermosensitive hydrogel containing vancomycin and a tri-enzymatic cocktail: *in vitro* and *in vivo* studies

Supplementary materials

Supplementary Figure 1. Influence of storage at 4°C on the activity of the TEC cocktail on a standard biofilm. The graph shows the percentage reduction in the biomass of a standard 24-h biofilm made by *S. aureus* MSSA 1144-20 and exposed to the enzymatic cocktail during 1 h. The graph compares the activity of a freshly prepared cocktail with that of the cocktail stored during 6 weeks at 4°C, expressed as percentage reduction in biofilm biomass.
Statistical analysis: unpaired t test. N=16 for each experimental condition.

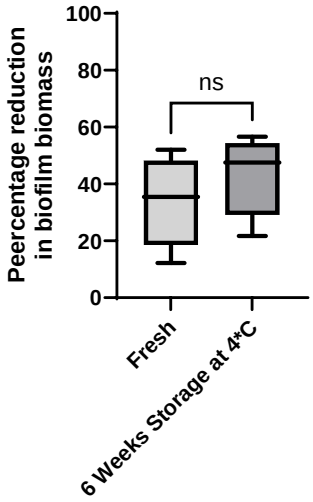

Supplementary Figure 2: Kinetics of protein release from poloxamer 407 and alginate hydrogels containing the TEC enzymatic cocktail and vancomycin (10 mg/mL). The total amount of proteins eluted (µg) was measured at 37°C over 7 days. Data are presented as mean ± SD (n = 3). Fitting curves and 80% release thresholds are shown.

Release from poloxamer was faster and more complete compared to alginate.

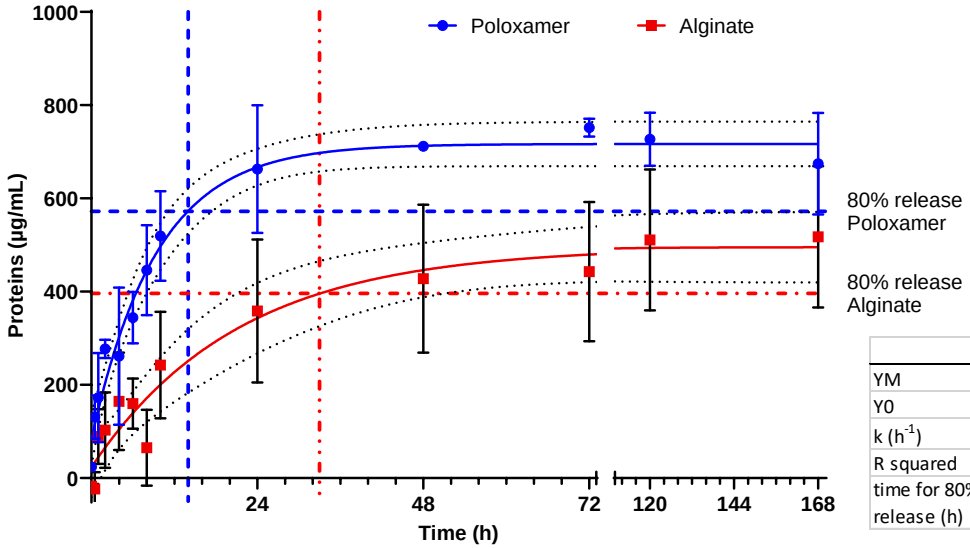

	Poloxamer	Alginate
YM	716.7	495.2
Y0	82.7	22.8
k (h^{-1})	0.106	0.04715
R squared	0.9058	0.7607
time for 80% release (h)	14.03	33.13

Supplementary Figure 3. Evolution of the weight of animals over the whole duration of the experiment. The graph shows the change (in percentage) of weight for animals from each experimental group over time. A reduction of 20% (dotted red line) is considered as a humane endpoint.

All animals gained weight during the experiments, the gain being significantly lower in group F as compared to non-infected animals (group A). Statistical analysis: 2-way ANOVA with Dunnett's post hoc test.

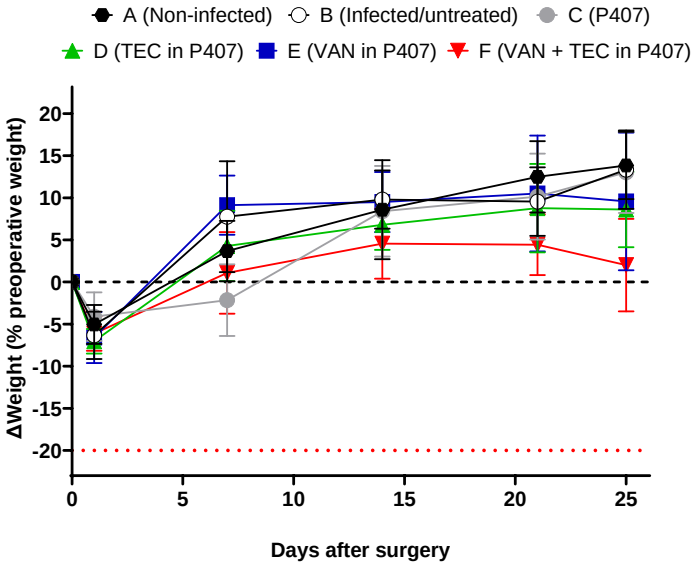

Supplementary Figure 4: Rheological characterization of poloxamer 407-based hydrogels with or without encapsulated agents (vancomycin [VAN, 10 mg/mL] and/or trienzymatic cocktail). (A) Temperature-dependent evolution of viscoelastic moduli (G′ and G″) as a function of temperature (10–40 °C), showing the sol-gel transition (Tgel, black arrow) for each formulation. **(B)** Comparison of Tgel values, defined as the temperature at which G′ ≥ G″. **(C)** Storage modulus G′ at 37 °C, reflecting the mechanical rigidity at physiological temperature. **(D)** G′ plateau values averaged between 35.5–38.5°C, indicating the stability of the gel post-transition. **(E)** Gelation kinetics (ΔG′/ΔT), calculated as the slope of G′ evolution within a ±2 °C window centred on Tgel. Data are shown as mean ± SD, with individual replicates (n = 3 per group). Statistical analysis was performed by one-way ANOVA or Kruskal-Wallis with post hoc correction (Dunnett). ns: not significant, *p < 0.05, ***p < 0.001. Rheological measurements were performed using a stress-controlled rotational rheometer under oscillatory mode (1 Hz, 1% strain) and a linear temperature ramp (1 °C/min). This multi-parametric analysis illustrates the influence of encapsulation on the sol-gel transition, post-gelling stiffness, and gelation kinetics, parameters relevant for biomedical injection and in situ gel formation.